Hindawi Publishing Corporation
International Journal of Photoenergy
Volume 2008, Article ID 258394, 19 pages
doi:10.1155/2008/258394

Review Article

Visible-Light-Active Titania Photocatalysts: The Case of N-Doped TiO_2s—Properties and Some Fundamental Issues

Alexei V. Emeline,[1] Vyacheslav N. Kuznetsov,[1] Vladimir K. Rybchuk,[1] and Nick Serpone[2]

[1] *Department of Photonics, Fock Research Institute of Physics, St. Petersburg State University, St. Petersburg, Russia*
[2] *Dipartimento di Chimica Organica, Universita di Pavia, Via Taramelli 10, 27100 Pavia, Italy*

Correspondence should be addressed to Nick Serpone, nick.serpone@unipv.it

Received 13 September 2007; Revised 14 October 2007; Accepted 12 November 2007

Recommended by M. Sabry A. Abdel-Mottaleb

This article briefly reviews some factors that have impacted heterogeneous photocatalysis with next generation TiO_2 photocatalysts, along with some issues of current debate in the fundamental understanding of the science that underpins the field. Preparative methods and some characteristics features of N-doped TiO_2 are presented and described briefly. At variance are experimental results and interpretations of X-ray photoelectron spectra (XPS) with regard to assignments of N 1s binding energies in N-doped TiO_2 systems. Relative to pristine nominally clean TiO_2 with absorption edges at 3.2 eV (anatase) and 3.0 eV (rutile), N-doped TiO_2s display red-shifted absorption edges into the visible spectral region. Several workers have surmised that the *(intrinsic) band gap* of TiO_2 is narrowed by coupling dopant energy states with valence band (VB) states, an inference based on DFT computations. With similar DFT computations, others concluded that red-shifted absorption edges originate from the presence of localized intragap dopant states above the upper level of the VB band. Recent analyses of absorption spectral features in the visible region for a large number of doped TiO_2 specimens, however, have suggested a common origin owing to the strong similarities of the absorption features, and this regardless of the preparative methods and the nature of the dopants. The next generation of (doped) TiO_2 photocatalysts should enhance overall process photoefficiencies (in some cases), since doped TiO_2s absorb a greater quantity of solar radiation. The fundamental science that underpins heterogeneous photocatalysis with the next generation of photocatalysts is a rich playing field ripe for further exploration.

1. INTRODUCTION

As a first-generation material, pristine TiO_2 has served well in the photoassisted (often dubiously referred to as photocatalytic) disposition of contaminants in aqueous and atmospheric ecosystems. The science that underlies heterogeneous photocatalysis has shown that the lowest energy level of the bottom of the conduction band (CB) of TiO_2 is a measure of the reduction potential of the photogenerated electrons, whereas the higher energy level of the valence band (VB) is a measure of the oxidation potential of photogenerated holes. pH-dependent flatband potentials, V_{fb}, of the CB and VB bands of this metal oxide determine the energy of electrons and holes at the interface. Accordingly, reductive and oxidative processes of couples with redox potentials more positive and more negative than the V_{fb} of CB and VB, respectively, can be driven by surface trapped electrons (e^-) and holes (h^+) that are poised to engage in various processes, the most important of which are photoreductions and photooxidations. An important issue regards the notion that once photogenerated, e^- and h^+ tend to recombine somewhat efficiently and rapidly relative to an otherwise slow redox chemistry at the TiO_2 surface. An additional, no less important issue is that TiO_2 absorbs a relatively small fraction (ca. 3–5%) of the solar radiation reaching the Earth's surface.

Of the two important polymorphs of TiO_2, anatase begins to absorb UV light around 387 nm (band gap energy, $E_{bg} \sim 3.2$ eV), whereas the absorption onset of rutile occurs around 413 nm ($E_{bg} \sim 3.0$ eV) increasing sharply to shorter wavelengths. Accordingly, in the late 1980s studies began to develop the next generation of titanium dioxides [1] that could absorb and make use of both UV (290–400 nm) and visible (400–700 nm) radiation to enhance process efficiencies. To achieve this feat required that the absorption edge

of TiO_2 be shifted to longer wavelengths (>400 nm). One way to accomplish this necessitated photosensitizing TiO_2 either with suitable dyes that unfortunately led to their own destruction, or with suitable metal-ion dopants that sometimes act as recombination centers of e^- and h^+; metal-ion dopants are often ineffective in aiding surface redox reactions, as appears to be the case when metal doping is achieved by wet impregnation [1]. However, metal-ion implantation methods have produced metal-doped TiO_2 specimens that enhance photoinduced surface processes even in the visible-light spectral region [2], where wet chemical methods failed.

First reports of anion-doped TiO_2, began to appear in the early 1990s, although Sato [3] had earlier hinted at a N-doped TiO_2. The 2001 study of Asahi and coworkers [4] on doping TiO_2 with various anions to prepare visible-light-active (VLA) N-doped TiO_2s was the catalyst needed to produce second-generation TiO_2 materials that are photoactive over the UV and much of the visible-light region. Subsequent studies reported several other visible-light-active N-doped TiO_2s, together with C-doped TiO_2 and S-doped TiO_2. The reports by Asahi et al. [4, 5] has led to a lively debate on the causes that lead the absorption onset of TiO_2 to be red-shifted to the visible region. They proposed that N-doping of TiO_2 red-shifts the absorption edge of TiO_2 and increases photoactivity by a *narrowing of the* TiO_2 *band gap*. Carbon- and sulfur-doped TiO_2 displayed similar red-shifts accompanied by increased photoactivity. As we will see later, others have proposed that electronic transitions in N-doped TiO_2 systems activated by visible-light irradiation involve transitions from N 2p localized states to the CB of TiO_2. Clearly, just as first-generation TiO_2 led to lively debates on the fundamental science that underpins TiO_2-assisted photoredox surface processes following photo-activation, so are the second-generation VLA TiO_2s generating enthusiastic discussions on the root cause that shifts the absorption onset to longer wavelengths. Three recent reviews have summarized some of the facets of first (undoped) and second generation (doped) titanias. [6–8].

This review article focuses briefly (a) on some preparative methods of visible-light-active N-doped TiO_2 materials and their XPS spectroscopic features, (b) on their visible absorption spectra that display the red-shift of the absorption edges, to terminate with (c) a brief visit into the lively debate concerning band gap narrowing.

2. NITROGEN-DOPED TiO_2s– SYNTHESES AND CHARACTERIZATION

Asahi et al. [4] initially set three requirements to achieve visible-light-activity for TiO_2: (i) doping should produce states in the band gap of TiO_2 that absorb visible light; (ii) the CB minimum and the dopant states of doped TiO_2 should be as high as or higher than the H_2/H_2O level to ensure photoreductive activity; and (iii) the intragap states should overlap sufficiently with the band states of TiO_2 to transfer photoexcited carriers to reactive sites at the TiO_2 surface within their lifetime. Metal dopants were undesirable because they did not meet conditions (ii) and (iii) as they produce localized *d* states deep in the band gap of TiO_2 and tend to act more as e^-/h^+ recombination centers. Calculations of density of states (DOS) of substitutional doping with several nonmetals (C, N, F, P, or S) into O sites in anatase TiO_2 by the full-potential linearized augmented plane-wave (FLAPW) formalism in the framework of the local density approximation (LDA) led Asahi et al. [4, 5] to choose N since the 2p states apparently contribute to band gap narrowing through mixing with O 2p states in the valence band. On the other hand, Yates and coworkers [9] classified the methods of synthesizing N-doped TiO_2s into (i) modification of existing TiO_2 by ion bombardment, (ii) modification of existing TiO_2 in powdered form, film, and single crystal, or else modify TiN by gas phase chemical impregnation, and (iii) grow $TiO_{2-x}N_x$ (crystals) from liquid or gaseous precursors.

Early on, Sato [3] had noted that calcination of $Ti(OH)_4$ in the presence of NH_4Cl (or aqueous NH_3) led to photosensitization of TiO_2 when exposed to visible-light radiation. The powdered samples were deduced to be NO_x-doped TiO_2 with the NO_x impurity acting as the sensitizer. Noda et al. [10] reported a yellow-colored anatase TiO_2 powder obtained from aqueous hydrazine and $TiCl_4$ solutions, and deduced that visible-light absorption was due to the presence of oxygen vacancies V_Os.

In their 2001 seminal report, Asahi et al. [4] prepared crystalline $TiO_{2-x}N_x$ films by sputtering a TiO_2 target in a N_2/Ar gas mixture followed by annealing at 550 C in a N_2 atmosphere. The yellowish $TiO_{2-x}N_x$ films absorbed light below 500 nm. X-ray photoelectron N 1s spectra (XPS) of the N-doped TiO_2 showed bands at 402, 400 and 396 eV; the undoped TiO_2 film showed no 396 eV band. The latter was assigned to atomic β-N in $TiO_{2-x}N_x$, whereas the 402-eV and 400-eV bands were attributed to molecularly chemisorbed dinitrogen γ-N_2 [11]. Powdered samples prepared with NH_3/Ar as the source of N followed by calcination at 550–600 C produced a $TiO_{2-x}N_x$ systems that showed XPS peaks at 396 eV; these systems were photoactive toward the decomposition of methylene blue (optimal loading, ~0.25 at.% N). The sites for photoactivity under visible-light irradiation were those when N substitutionally replaced O, that is, sites associated with atomic β-N at 396 eV [4]. Lee et al. [12] fabricated N-doped TiO_2 anatase films by MOCVD using $Ti(i\text{-}PrO)_4$ and N_2O at 420 C; XPS Ti 2p spectra showed N was incorporated into the TiO_2 lattice to form Ti–N bonds. Hydrolysis of $Ti(SO_4)_2$ with NH_3 in dry air at 400 C produced a visible-light-active anatase TiO_2 ($\lambda < 550$ nm) [13]; however, XPS spectra showed only trace amounts of N, with visible-light response due to an oxygen-deficient stoichiometry.

Pale yellow, yellow, and dark green $TiO_{2-x}N_x$ ($x = 0, 0.0050, 0.011, 0.019$) powdered samples can be prepared by annealing anatase TiO_2 powder (ST-01) in a flow of NH_3 at 550, 575, and 600 C, respectively [14]. XRD patterns indicated that the samples retain the anatase structure; no TiN phase was present. The XPS peak at 396 eV confirmed substitutional N doping of O sites yielding O–Ti–NO bonds. Noticeable shifts of the absorption edge into the visible spectral region were evident for $TiO_{2-x}N_x$. The feature at $\lambda > 550$ nm was attributed to Ti^{3+} since NH_3 decomposes into N_2 and H_2 at ca. 550 C, and H_2 reduces Ti^{4+} under these conditions.

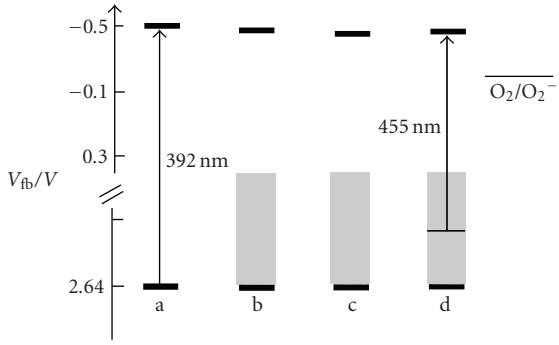

Figure 1: Electrochemical potentials (versus NHE) of band edges of three N-doped TiO_2s: (a) TiO_2, (b) TiO_2–N/1, (c) TiO_2–N/2, (d) TiO_2–N/3. Shaded areas denote surface states; the oxygen redox potential at pH 7 is also shown. Reproduced with permission from [16]. Copyright Wiley-VCH Verlag GmbH & Co. KGaA.

The band gap energy remained at 3.2 eV. Mineralization of isopropanol to CO_2 with UV-light and visible-light radiations resulted in different quantum yields, suggesting that N-doping forms a narrow N 2p band above the valence band of TiO_2. Note that band gap narrowing in $TiO_{2-x}N_x$, as inferred by Asahi et al. [4], would have required identical quantum yields. On irradiating with visible light, the quantum yields decreased with increase in x of the dopant N because of the increase in oxygen vacancies, V_Os, with increase of x in $TiO_{2-x}N_x$. In this case, V_Os act as recombination centers for e^- and h^+. Under UV irradiation, the quantum yields also decreased with increase in x, suggesting that the doping sites also act as recombination centers.

Nanocrystalline porous N-doped TiO_2 thin films, prepared by introducing N into anatase TiO_2 by means of DC magnetron sputtering in N_2-containing plasma [15], displays new spectral features in the spectral range $410 < \lambda < 535$ nm at low N concentrations owing to excitation of e^- to unoccupied states from local states located slightly above the VB edge. N-doping had no effect on the conduction band edge. Band gap narrowing was deemed somewhat questionable by these authors [15]. Despite the intense recombination of charge carriers caused by N-doping, the new band gap states created by N-doping improved the visible-light photoresponse at the expense of some losses of the UV response.

Sakthivel and Kisch [16] prepared yellow N-doped anatase TiO_2 with various N loadings by hydrolysis of $TiCl_4$ with a N-containing base {aqueous NH_3, $(NH_4)_2CO_3$ or NH_4HCO_3} followed by calcination at 400 C. XPS spectra showed only a broad signal at ∼404 eV (but no 396-eV peak) attributed to the hyponitrite (NO^-) species that was confirmed by infrared spectral techniques. No changes in the valence band edge occurred on N-doping, despite the red-shift of the TiO_2 absorption edge to ∼250 nm . Contrary to the inference by Lindgren et al. [15], however, photoelectrochemical results [16] showed a slight change in the electrochemical potentials of the CB of TiO_2 (see Figure 1) for three of the specimens. According to the authors [16], N-doping led only to a "modest band gap narrowing."

High-energy ball milling of P-25 TiO_2 (ca. 80% anatase and ∼20% rutile) with various quantities of hexamethylenetetramine (HMT) at near-ambient temperatures yields yellowish N-doped rutile TiO_2 [17], which subsequent to calcination in air at 400 C gives an N-doped product that displays absorption edges at ∼400 and 550 nm and a good visible-light photoresponse toward oxidation of NO.

Ion-assisted electron-beam evaporation of rutile titania powder and N_2 yields crystalline anatase $TiO_{2-x}N_x$ films with a considerable amount of substitutional N atoms (1.8 at.%) and chemisorbed molecular N_2 [18]. XPS spectra showed peaks at 402 and 396 eV assigned to molecularly chemisorbed γ-N_2 and atomic β-N, respectively; Ti 2p XPS spectra revealed Ti^{4+} $2p_{3/2}$ and Ti^{4+} $2p_{1/2}$ in the anatase TiO_2 film indicating that the majority of titanium in the $TiO_{2-x}N_x$ film consisted of Ti^{4+}, thus confirming the results of XRD patterns. N-doping caused no changes to the anatase TiO_2 structure as attested by Raman spectroscopy.

In a simplified synthesis, Gole and coworkers [19, 20] produced $TiO_{2-x}N_x$ samples at room temperature using direct nitridation of anatase TiO_2 with alkylammonium salts. The samples could be tuned to respond to wavelengths up to λ∼550 nm. The method first yielded metal-oxide colloids by the controlled hydrolysis of Ti(i-PrO)$_4$ in aqueous/isopropanol media (pH 2; HNO_3), subsequent to which treatment in excess $(C_2H_5)_3N$ led to $TiO_{2-x}N_x$ nanocolloids. XRD and HRTEM results demonstrated that the treated $TiO_{2-x}N_x$ nanoparticles were predominantly anatase. Diffuse reflectance spectra (DRS) of the $TiO_{2-x}N_x$ crystallites rose sharply at ∼450 nm ; the corresponding DRS spectrum of nitrided $TiO_{2-x}N_x$ from partially agglomerated nanoparticles rose at ∼550 nm. XPS analysis with Ar^+-ion sputtering revealed the presence of N dopants at the surface and in the sub-layers of $TiO_{2-x}N_x$ agglomerates (N content, 3.6–5.1 at.%). No evidence was found for conversion of the anatase structure into rutile on N-doping for the initial TiO_2 nanocolloids and for the agglomerated gel solutions. Little if any XPS evidence of atomic β-N binding at 396 eV was found in any of the $TiO_{2-x}N_x$ samples. Rather, the XPS results were consistent with nonstoichiometric surface-based Ti–O–N bonding.

In a later related detailed XPS study of a series of TiO_2-based nanometer-sized photocatalysts that included nitrogen-doped TiO_2 nanoparticles, Chen and Burda [21] noted a broad N 1s binding energy peak of the nitrogen-doped TiO_2 nanoparticles that was centered at ca. 401.3 eV (see Figure 2) and extended from 397.4 eV to 403.7 eV, a range greater than the typical binding energy of 397.2 eV in titanium nitride, TiN. These findings were attributed to the formation of an O–Ti–N structure that was suggested as the chemical entity formed during the substitutional doping process and responsible for the significant increase in photocatalytic activity of synthesized nitrogen-doped nanoparticles. Moreover, the XPS observations reported by Chen and Burda [21] were not consistent with a Ti-N entity within the TiO_2 nanocolloid lattice [22]. The shift in the N 1s binding energy for the $TiO_{2-x}N_x$ nanocolloid to higher energies relative to TiN was likely due to a more positive oxidation state of nitrogen in relation to the N 1s binding energy in

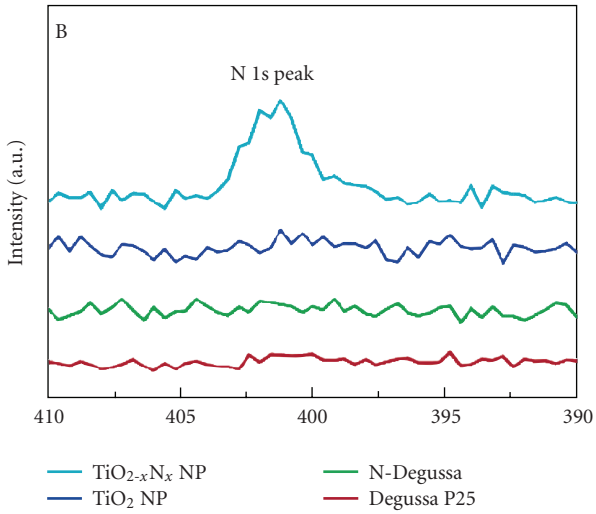

Figure 2: X-ray photoelectron spectra of various TiO_2 specimens; N-Degussa is nitrided P25 TiO_2 and $TiO_{2-x}N_x$ NP denotes $TiO_{2-x}N_x$ nanoparticles. Reproduced with permission from [21]. Copyright (2004) American Chemical Society.

$NaNO_3$ (408 eV), in NH_3 (398.8 eV) and adsorbed NO (400–401.5 eV) [23]. Attribution of the N 1s peak at 400 eV to γ-N_2 in N-doped titanias has been questioned by Chen et al. [23] in that N_2 is not chemisorbed on metal oxides such as TiO_2 at ambient temperature, preferring instead to assign the 400 eV peak to NO species consistent with the attendant heat release on the creation of these sites in the TiO_2 lattice.

Gopinath [24] recently questioned the validity of the conclusions reached by Chen and Burda [21] as not being consistent with the reported XPS observations, suggesting (among others) rather that there may have been surface contamination of the analyzed nanocolloidal N-doped TiO_2 material as a result of atmospheric degradation. Based on earlier studies of XPS spectra of NH_3 and primary alkyl/aromatic amines (398–399 eV), anionic N^{3-} in TiN (396–397 eV), adsorbed NO and NO_2 on ZnO (401 and 405 eV, resp.) and Sato and coworkers' [25] observation of the N 1s core level at 400 eV for N-doped TiO_2 prepared by a wet method and attributed to an impurity sensitization such as NO, Gopinath [24] argued that the 401.3-eV peak in the N–TiO_2 nanocolloid reported by Chen and Burda [21] was more likely due to oxidized nitrogen as in N–O–Ti–O or O–N–Ti-O, and that the high binding energy of 401.3 eV was associated with some partial positive charge on N as noted by György and coworkers [26] in the nitridation of titanium for the 400–401 eV peak attributed to an O–N–Ti structure. Also questioned by Gopinath [24] were the origins of the O 1s core levels at binding energies of 530 and 532 eV ascribed by Chen and Burda [21] to O-Ti-O and to N-Ti-O structural units, respectively. Gopinath [24] insisted that the 532-eV peak was likely due to surface contamination by some carbon oxide, such as CO_2, and further claimed that the large level of N-doping in nanocolloids (ca. 4–8%) was rather unlikely. In an appropriate response, Burda and Gole [27] pointed out that Chen and Burda [21] used the shorthand notation N – Ti – O to mean that N, Ti, and O were bound to next neighboring atoms (Ti or O) in the TiO_2 lattice and *not* to mean an isolated triatomic molecular species with a nonoxidized nitrogen, and were thus rather surprised by Gopinath's misinterpretation since such notation was chemically obvious even to others [28]—also see below. In fact, as clearly stated by the groups of Gole and Burda [19, 20, 22, 23] the discussion dealt with a minimal structure fragment within a doped TiO_2 lattice (characterized by NO sites), and *not* some species where the nitrogen was not oxidized. As well, the apparent discrepancy noted by Gopinath [24] in the XPS data reported earlier by others (see refs 13–20 in [27]) did not take into account that the data were taken under vastly different conditions across distinct physical entities that included films and undoped nanoparticles, not to mention the anatase and rutile structures. Burda and Gole [27] further noted that Gopinath's misinterpretation of their studies originated with the misconception that N, Ti, and O are isolated from their TiO_2 anatase environment, when in fact the XPS results reported by Chen and Burda [21] clearly demonstrated that nitrogen was partially oxidized and that the neighboring Ti was reduced relative to Ti in pure TiO_2. The discussion concerning the valencies of the nitrogen had indeed attributed the 401-eV peak to an NO site [22, 23]; however, the precise location of the NO site within the titania lattice remains a subject yet to clarify. Finally, that the doping levels are as high as 4 to 8% in the N-doped TiO_2 colloids are not unusual based on nucleophilic substitution chemistry, as pointed out previously [23].

The above reports, misinterpretations and misunderstandings, together with other XPS results described below, clearly demonstrate that XPS results do not in themselves provide unequivocal understanding of the exact nature of N-doped titania specimens, not to mention the nature of other anion- and cation-doped TiO_2s.

Nakamura and coworkers [29] produced anatase $TiO_{2-x}N_x$ materials by two methods: (a) in the dry method anatase ST-01 TiO_2 was heated to 550 C in a dry NH_3 flow and (b) in the wet method the $Ti(i\text{-}PrO)_4$ precursor was hydrolyzed in aqueous NH_3 at 0 C followed by calcination at 400 C. Nitrogen-doped nanocrystalline TiO_2 (yellow) powders have also been synthesized by a procedure developed by Ma and coworkers [30]. Commercial anatase ST-01 TiO_2 heated at 500 C under a dry N_2 gas flow in the presence of a small quantity of carbon also yields N-doped yellow TiO_2 whose XRD patterns reveal the sample to have the anatase structure, even after annealing at 500 C. XPS spectra showed peaks at 396.2, 398.3, and 400.4-eV in the N 1s region, with the first two peaks attributed to chemically bound N-species and to O–Ti–N linkages within the crystalline TiO_2 lattice, respectively, whereas the 400.4-eV peak was ascribed to molecularly chemisorbed N_2 species.

Ion implantation of atomically clean TiO_2 (110) surfaces in single crystals with mixtures of N_2^+ and Ar^+ ions, followed by subsequent annealing under ultrahigh-vacuum conditions, led to incorporation of N into the TiO_2 lattice [31]. XPS spectra revealed only the N 1s feature at 396.6 eV attributed to substitutionally bound nitride nitrogen (O^{2-} ions substituted by N^{2-} anions). Contrary to expectations,

N-doped crystals containing only nitride ions exhibited a shift in the photothreshold energy of 0.2 eV to *higher* (shorter wavelengths) rather than *lower* (longer wavelengths) *energy* compared to undoped TiO_2 (110). N-doped TiO_2 (110) rutile single crystals previously treated in the presence of an NH_3/Ar gas mixture at ca 600 C exhibited photoactivity at the *lower photon energy* of 2.4 eV, that is, 0.6 eV below the band gap energy of rutile TiO_2 (3.0 eV) [32]. The active dopant state of the interstitial N responsible for this effect showed a N 1s binding energy at 399.6 eV attributed to a form of nitrogen likely bound to H. This is distinctively different from the substitutional nitride state, which displays a N 1s binding energy at 396.7 eV. Apparently a co-doping effect of N and H probably enhanced the visible-light photoactivity. Doped and undoped TiO_2 (110) samples also showed an impurity XPS feature at 399.6 eV, which on UV treatment in air and/or Ar^+-ion sputtering led to extensive depletion of the signal indicating that traces of nitrogen may have contaminated the metal-oxide surface. Such inferences by the Yates group are in stark contrast to those of Asahi et al. [4] and those of others who claimed that nitridic nitrogens that substitute O^{2-} ions in the TiO_2 lattice are the necessary dopant species for TiO_2 photoactivity in the visible-light spectral region.

In a later study, Thompson and Yates [33] re-emphasized that the exclusive XPS N 1s signal at 396.7 eV attributed to substitutional β-N in ion-implanted N-doped TiO_2 does not account for the *decrease* in the photothreshold of TiO_2 (110), as observed for interstitially located N–H bound species. Rather, they pointed out that the 0.2-eV *increase* in photothreshold energy of N-doped TiO_2 systems arose from deposition of charge in the low levels of the CB (the band-filling mechanism). Although clear XPS evidence exists for the incorporation of β-substitutional N in N-doped TiO_2, there is no strong and firm evidence of any appreciable photoactivity when these doped systems are irradiated with visible light according to Yates et al. [9], a point also raised by Frach et al. [34] who further noted no improvement in visible-light activity on N-doping TiO_2, and by Li and coworkers [35] who reported that the nature and level of visible-light activity depended on the nitriding compound employed.

With $TiCl_4$, ethyl acetate and NH_3 as precursors and N_2 as the carrier gas, Yates and coworkers [9] used an atmospheric pressure thermal CVD coater to grow thin films of N-doped TiO_2 on glass substrates. Only three grown samples displayed the XPS N 1s peak at 396 eV of atomic β-substituted N. XPS N 1s spectra showed no evidence of the 397-eV signal typically due to the N^{3-} ion (TiN), but did reveal weak signals at 400 and 402 eV probably arising from molecularly chemisorbed N_2, or from NH_x species located at interstitial sites (399.6 eV), or from NO_x, or NH_x (400 eV), or from an oxynitride (399.3 eV) of stoichiometry equivalent to $TiN_{0.5}O_{0.5}$. Some of the films displayed visible spectral absorption features, but so did nominally undoped TiO_2 films indicating that N incorporation cannot be assumed on the basis of red-shifts of the absorption edge. Even though the N-doped TiO_2 specimens revealed the presence of β-N incorporation and absorption spectral features in the visible region, they were photo-inactive under visible light irradiation, while the UV photoactivity was reduced considerably compared to films grown in the absence of NH_3. Clearly, the presence of β-nitrogen alone cannot be claimed to induce visible-light activity in N-doped TiO_2 films, a point also raised by Mrowetz and coworkers [36] who prepared two different yellow-colored N-doped TiO_2 samples: *sample A* prepared by the method of Gole et al. [19, 20] and *sample H* prepared by the high-temperature nitridation of commercial anatase TiO_2 at 550 C in a NH_3/Ar gas flow. XPS spectra of sample *A* surface revealed intense peaks at 399.6 and 404.5 eV in the N 1s region, whereas the peak at 396 eV in the XPS spectra of sample *H* powders was weak and diffuse, even after Ar^+-ion sputtering. Despite these observations, the N-doped TiO_2 materials *failed to catalyze* the oxidation of $HCOO^-$ to $CO_2^{-\bullet}$, and NH_3–OH to NO_3^- under visible-light illumination.

The solvothermal process using a $TiCl_3$/HMT/alcohol (methanol or ethanol) mixed solution in an autoclave at 90 C and then at 190 C yields N-doped TiO_2 nanoparticles consisting of pure anatase (pH 9, methanol), rutile (pH 9, ethanol) and brookite (pH 1, methanol) phases, which showed good visible-light absorption and visible-light activity at $\lambda > 510$ nm [37]. The two-step absorption in the reported diffuse reflectance spectra (DRS) became apparent only after calcination at 400 C. The first absorption edge is related to the band structure of nondoped TiO_2, whereas the second absorption edge around 520–535 nm is due to the formation of a N 2p band located above the O 2p valence band in the $TiO_{2-x}N_x$ specimen.

Electrochemical anodization of titanium in HF/H_2SO_4 electrolyte, followed by calcination at different temperatures (range 300–600 C) in pure NH_3, yields self-organized N-doped TiO_2 nanotubes [38]. The initial amorphous nanotubes were converted to anatase, with some rutile present depending on the heat-treatment temperature. Absorption spectra of the $TiO_{2-x}N_x$ nanotubes displayed a sub-band gap energy of ~2.2 eV (that may be referred to as an *extrinsic band gap*) and the *intrinsic band gap* of anatase (~3.2 eV). The N 1s XPS spectrum showed two clear peaks, one at 400 eV, ascribed to molecularly chemisorbed dinitrogen (γ-N_2 state), and the other at 396 eV, attributed to the atomic β-N state.

The RF-MS deposition method produces N-substituted $TiO_2\{N\text{–}TiO_2(X)\}$ photoactive thin films using various N_2/Ar mixtures as the sputtering gas ($X = 2, 4, 10, 40$) and a calcined TiO_2 plate as the source material [39]. The absorption edge of the films red-shifted to 550 nm, with the extent of the shift depending on the concentration of N(X) substituted within the TiO_2 lattice (range 2.0–16.5%). The specimen with 6.0% N exhibited the highest visible-light activity in the photooxidation of isopropanol (aqueous media; irradiation $\lambda \geq 450$ nm), and the photooxidation of H_2O (irradiation $\lambda \leq 550$ nm). XPS and XRD measurements showed significant substitution of lattice O atoms of TiO_2 by N atoms, which Kitano and coworkers [39] suggested as playing a crucial role in the *band gap narrowing* of the TiO_2 thin films (range 2.58–2.25 eV relative to 3.2 eV, depending on X) enabling the visible-light photoresponse. In samples with $X > 4$, the Ti^{3+} species formed in the N–$TiO_2(X)$ samples

acted as recombination centers of e^- and h^+ and thus led to a decreased photoactivity.

Joung et al. [40] used the hydrolysis of Ti(i–PrO)$_4$ in anhydrous ethanol containing HCl, followed by treatment of the resulting colloids in an NH_3 stream at 400 C, 500 C and 600 C at various time intervals (5 to 60 min) to prepare visible-light-active N-doped TiO_2 materials. The highest photoactivities were seen for samples prepared at 400 C and 600 C and calcination times of 5 and 10 min, whereas for samples prepared at 500 C the highest photoactivity was observed for a calcination time of 60 min. XRD patterns of the TiO_2 powders before and after N-doping showed that N-doping caused no changes to the anatase phase. The N 1s XPS spectra of the $TiO_{2-x}N_x$ samples displayed a peak at 399.95 eV that was tentatively assigned to adsorbed NO or to N in Ti–O–N; however, no peak attributable to Ti–N bonding at 396 eV was observed. Band gap energies of N-doped TiO_2 inferred from absorption spectra ranged from 2.92 to 3.04 eV, for samples prepared at 400 C (5 min) and at 500 C (60 min), respectively. For samples prepared at 400 C (5 and 10 min), the active species were described as being NO, NO_2, NO_2^-, NH_2, whereas for samples prepared at 500 C (60 min) the active species was identified as doped atomic N; the active species for samples prepared at 600 C (5 and 10 min) were inferred to be doped atomic N along with NO, NO_2, NO_2^-, and NH_2 species.

At this time, it is important to realize that visible-light photoactivity of N-doped TiO_2 materials appears to be highly sensitive to the preparative routes, because although such materials may absorb visible light, they are nonetheless frequently inactive in photooxidations. To the extent that photogenerated charge carriers in and by themselves do not impart photoactvity and that charge carrier recombination must be muted to allow the carriers to reach the metal-oxide surface, In and coworkers [41] prepared a series of $TiO_{2-x}N_x$ systems with nominal N loadings from 0.2 to 1.0 wt.% involving the sequential reaction of H_2O with a small known excess of $TiCl_4$ in toluene (step 1) under dry O_2-free argon, followed by the stoichiometric reaction of the remaining $TiCl_4$ with a standard solution of NH_3 in dioxane (step 2). The resulting species were heat-treated in air at 400, 500, and 600 C. Tests of the $TiO_{2-x}N_x$ specimens for visible-light photoactivity revealed (i) that calcination at 400 C yields a solid with pronounced absorption in the visible spectral region but yet no visible-light photoactivity, (ii) that 500 C calcination produces an effective (yellow) visible-light-active sample, and (iii) that the heat treatment at 600 C results in an inactive white material.

In two extensive reports, Belver and coworkers [42, 43] prepared and characterized a series of nanosized N-doped TiO_2-based materials by a reverse micelle microemulsion method using a Ti(i-PrO)$_4$ precursor and three N sources, for example, 2-methoxyethylamine, N,N,N',N'-tetramethylethylenediamine and 1,2-phenylenediamine, to produce Ti(IV) complexes in dry isopropanol under a N_2 atmosphere. Dropwise addition of the solution to the inverse microemulsion, that contained H_2O dispersed in n-heptane and Triton X-100 as the surfactant with hexanol as the cosurfactant, produced materials that were subsequently calcined at 200 C and then at 450 C. A XANES examination confirmed the anatase structure of $TiO_{2-x}N_x$. XANES spectra also showed a lack of correlation between the number of oxygen vacancies (V_Os) and the N content in the samples. Above a certain limit, the association of point defects, such as V_Os and/or the presence of nonpoint extended defects, was detrimental to photoactivity. The distribution of defects and the nature of defects present in the N-doped samples were examined in a joint XANES/EXAFS investigation, which revealed that the distribution of defects was not simply related to the oxygen vacancies V_Os, since strong differences existed in the first cation-cation coordination shell that inferred the possible presence of nonpoint defects. The joint study also confirmed the point defects to be the V_Os; no interstitial defects were seen and the O/Ti atom ratio was <2. Evidently, there exists an optimal O/Ti ratio for maximum photoactivity achieved when oxygen vacancies are located in the bulk lattice that act as electron traps subsequent to visible-light photoactivation of the doped specimens. No apparent effect due to N-doping on the valence band edge was detected. Some localized states were, however, detected at the bottom of the conduction band with broad absorption around 500 nm. Results from DRIFT spectra indicated the presence of several anion-related impurities of a substitutional (N^{n-}) and interstitial (NO^+) nature. Although these species contributed to the absorption features, the authors [42, 43] found no clear correlation between any of these species and photoactivity. In fact, photoactivity best correlated with an optimal number of oxygen vacancies, above and below which a decrease of steady-state reaction rates occurred.

N-doped titania samples with high visible-light activity have been synthesized using a layered titania/isostearate nanocomposite from a sol-gel technique [44], with N-doping achieved by treating the composite with aqueous NH_3 followed by calcination either in an O_2/N_2 mixture or in pure N_2 at various temperatures (300, 350, 400, 450, and 500 C). The vivid yellow samples absorbed visible light in the 380–500 nm spectral region, and correlated with the extent of doped-N content in the samples. However, the visible-light photoactivity *did not correlate* with N content. The highest visible-light photoactivity was observed for the 400-C calcined sample. The quantity of N content in the sample decreased on increasing the calcination temperature, which was particularly significant between 300 and 350 C, with the decrease being more important for the sample calcined in O_2/N_2 than for the sample calcined in pure N_2.

Thus far we have witnessed that visible-light-active (VLA) TiO_2 systems doped with nitrogen possess, in most cases, good attributes toward the photooxidation of organic and inorganic (e.g., NO_x) substrates. Of particular interest have been the materials doped with N whose preparative methods have been varied but otherwise simple in a large number of cases. Most important, however, although all the N-doped TiO_2 materials displayed absorption features and absorption edges red-shifted to the visible spectral region (at least to 550 nm), photoactivity of these systems under visible-light irradiation has not always correlated with these absorption features. In a recent study, Tachikawa and coworkers [45] addressed some of these issues and described

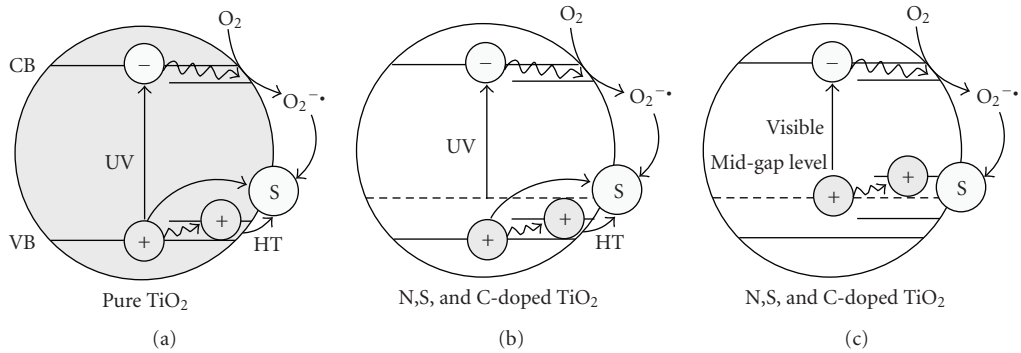

Figure 3: Cartoons illustrating possible photoassisted processes of a substrate adsorbed on the surfaces of pure, N-, S-, and C-doped TiO_2 nanoparticles. Reproduced with permission from [45]. Copyright (2007) American Chemical Society.

mechanisms of the photoactivity of VLA TiO_2 specimens. Using solid-state NMR measurements combined with transient diffuse reflectance (TDR) spectroscopy, these workers provided direct evidence of the degradation of ethylene glycol with VLA-active $TiO_{2-x}N_x$ under visible-light irradiation. It appears that photoassisted oxidations of organic compounds on the surface of $TiO_{2-x}N_x$ proceed by surface intermediates generated from oxygen reduction (the superoxide radical anion, $O_2^{-\bullet}$) or otherwise water oxidation (the •OH radical) *and not* by direct reaction with h^+ that may be trapped at the N-induced mid-gap level (see Figure 3). Based on their experimental results, it is rather evident that *both* an appropriate *lower-energy photo-threshold* for visible-light absorption and *high carrier mobilities* are needed for advanced visible light-active TiO_2-based photocatalysts.

3. DFT COMPUTATIONS OF BAND GAP ENERGIES IN N-DOPED TiO_2

Different preparative methods and strategies of N-doping TiO_2 as described above can lead to anion-doped metal-oxide materials with entirely different properties—these are the next generation TiO_2 photocatalysts. The key question that keeps recurring in the literature is the chemical nature and the location of the species that lead(s) the absorption edge of TiO_2 to be red-shifted and consequently to the visible-light activity of doped TiO_2. Species such as NO_x, NH_x, and N^{2-} have been proposed, not to mention NO^-, NO_2^- and NO_3^- species that have been confirmed experimentally. Another key question regards the electronic structure(s) of the (anion)-doped materials and their fate when subjected to UV- and/or visible-light irradiation. Although, these questions have been addressed in several interesting computational studies, a consensual acceptance of the results has yet to be reached. Significant advances can be made in clarifying key questions by a combination of experimental and computational studies within the same laboratory or among collaborating laboratories.

Densities of states in anatase TiO_2 for substitutional doping of oxygen in the lattice by C, N, F, P, and S dopants were first reported by Asahi and coworkers [4, 46] using the *full-potential linearized augmented plane-wave* (FLAPW) formalism in the framework of the *local density approximation* (LDA). The calculations were carried out without geometry optimization for the five anion-dopings because the resulting atomic forces were apparently too large to obtain reasonable positions in the unit cell (eight TiO_2 units per cell). Three types of doping for N were considered in the computations: (a) substitutional N doping (N_S), (b) interstitial N doping (N_I), and (c) both types of doping (N_{S+I}) in the anatase TiO_2 architecture. Optimization of the N positions in the cell inferred molecularly bonding states (NO and N_2) for cases (b) and (c) with bond lengths (improved by the *generalized gradient approximation* GGA) in fair agreement with accepted values: 1.20 A *versus* 1.15 A (N–O) and 1.16 A *versus* 1.10 A (N_2). According to the authors [4], substitutional doping of N was the most effective because its 2p states contribute to band gap narrowing by mixing with O 2p states of the valence band. Calculated imaginary parts of the dielectric functions of $TiO_{2-x}N_x$ showed a shift of the absorption edge to lower energy by N doping, with dominant transitions from N $2p_\pi \rightarrow$ Ti d_{xy} rather than from O $2p_\pi$ as in TiO_2. However, the calculated band gap energies were considerably underestimated relative to the experimental value (e.g., E_{bg} = 2.0 eV *versus* 3.2 eV for anatase) attributed, in part, to the well-known shortcomings of the LDA approach. The underestimated band gap was corrected using a scissors operator (a sort of *fudge factor*) that displaces the empty and occupied bands relative to each other by a rigid shift of 1.14 eV to bring the minimum band gap in line with experiment for the band gap of anatase TiO_2 (corrected E_{bg} = 3.14 eV). Accordingly, the band gaps of N-doped $TiO_{2-x}N_x$ systems were also adjusted by the factor 1.14 eV [4] on the assumption that the underestimated energy of the band gap in the LDA approach is not affected by N-doping because long-range screening properties in $TiO_{2-x}N_x$ were likely similar to those in TiO_2.

The picture as to the exact cause of the red-shift of the absorption edge of TiO_2 in various N-doped TiO_2 (*anatase*) powders becomes somewhat confused with the report from Yates group [30] that the absorption edge of a N-doped TiO_2 *rutile* single crystal shifts to higher energy by 0.20 eV. Spin-polarized density functional theory (DFT) calculations within the GGA approximation by Di Valentin and coworkers [47] showed that whereas in anatase the localized N 2p

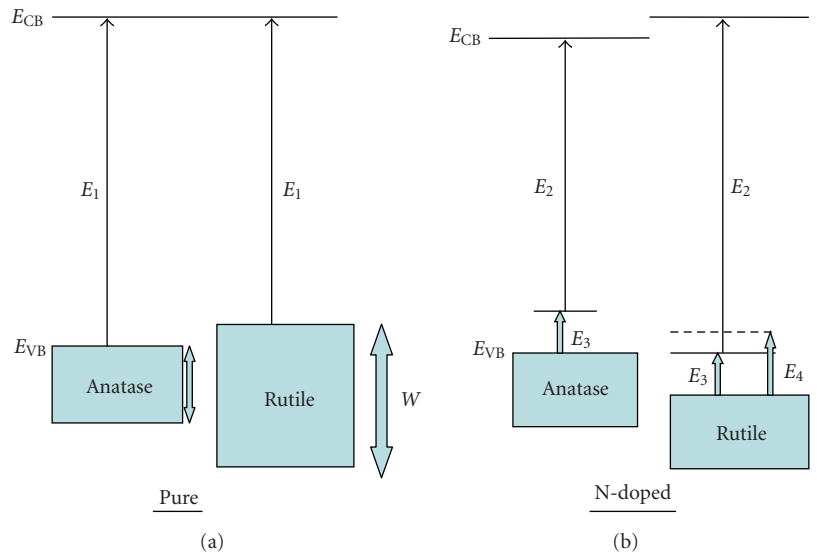

Figure 4: Schematic representation of the energy band structure of pure and N-doped anatase and rutile (energies not to scale). Note the modest shift of 0.03 eV in E_C of the conduction band to higher energies and the contraction energy E_4 in the N-doped rutile TiO_2. E_3 represents the energy of the N dopant levels above the valence band. Higher levels of doping, for example, three N atoms per supercell, cause a small shift of ~0.05 eV to higher energies for E_C which is overcompensated by the presence of N-derived states just above VB, so that the excitation energy E_2 from these states to the conduction band is reduced by <0.1 eV compared to pure anatase (W denotes the width of the valence bands). Adapted from results reported in [47].

states, located just above the O 2p states of the valence band, red-shift the absorption edge to lower energy, in rutile the tendency to red-shift the absorption edge is offset by a concomitant contraction of the O 2p valence band resulting in an overall increase in the optical transition energy by ca. 0.08 eV. Compared to anatase, rutile has a wider (W) O 2p band due to both its higher density and its different structure (see Figure 4). In this work [47], N-doping was modeled by replacing 1, 2, or 3 oxygen atoms in a 96-atom anatase supercell and 1 or 2 oxygen atoms in a 72-atom rutile supercell giving a stoichiometry comparable to that used in experiments for $TiO_{2-x}N_x$: $0.031 < x < 0.094$ for anatase and $0.042 < x < 0.084$ for rutile. Note that Asahi et al. [4, 46] used a higher level of N-doping, which yielded a stoichiometry of $TiO_{1.875}N_{0.125}$. Inclusion of more N atoms in the same supercell yielded more accurate results than using smaller supercells. Nonetheless, calculated band gaps [47] were still underestimated at 2.19 eV and 1.81 eV (at the Γ position) *versus* the experimental 3.2 eV and 3.0 eV, respectively, for pure undoped anatase and rutile TiO_2, again because of the shortcomings of the DFT method. Analysis of the electronic energy levels (see Figure 4) shows that N-doping causes no shift of the position of both top and bottom of the O 2p VB band and of the CB band relative to pure undoped anatase TiO_2, in significant contrast with the conclusions of Asahi and coworkers [4, 46] with respect to the undoped material. Structural variations in rutile TiO_2 subsequent to substitution of one O atom with N in the 72-atom supercell appear significant in rutile relative to anatase in which the variations were inconsequential. In any case, the N impurity states can act as deep electron traps in $TiO_{2-x}N_x$ systems (see Figure 4). Di Valentin et al. [47] also considered the contribution of oxygen vacancies (V_Os), estimated experimentally at 0.75 to 1.18 eV below the conduction band E_C (DFT calculations placed them at 0.3 eV below E_C), to the overall visible-light photoactivity of N-doped systems when V_Os trap electrons to produce F-type color centers. The simultaneous presence of N dopants and V_Os can also lead to charge transfer states (reaction 1) that can further contribute to the visible-light photoactivity,

$$V_O(F) + N \longrightarrow V_O^{\bullet}(F^+) + N^-. \quad (1)$$

In a later study that combined experiments (EPR, XPS) and DFT calculations performed using the plane-wave-pseudopotential approach, together with the Perdew-Burke-Ernzerhof (PBE) exchange correlation functional and ultrasoft pseudo-potentials, Di Valentin and coworkers [48] characterized the paramagnetic species present in N-doped anatase TiO_2 powders obtained by sol-gel synthesis, and unraveled some of the mechanistic details of the visible-light activity of N-doped TiO_2 as to whether photoactivity is due to NO_x or NH_x species or simply to substitutional N-doping. The $TiO_{2-x}N_x$ sample was obtained by hydrolysis of $Ti(i\text{-}PrO)_4$ in isopropanol media in the presence of aqueous NH_4Cl as the N source, followed by calcinations of the N-doped specimen at ca. 500 C for 2 hrs. XPS N 1s spectra showed only a peak at ca. 400 eV attributed to interstitial N (without precluding others); no 396 eV peak was seen that might have originated from substitutional N-doping. EPR spectra indicated the presence of two different paramagnetic species that were attributed to substitutional and interstitial N species. These results led them to consider two structurally different locations for the N dopant in their DFT calculations: substitutional N(N_S) and interstitial N(N_I) atoms in

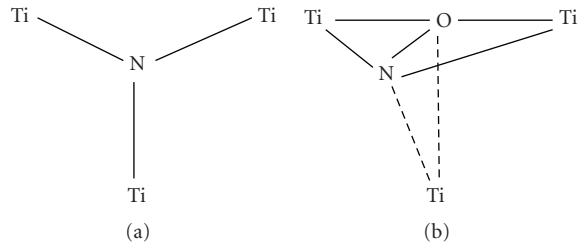

Figure 5

the TiO_2 anatase matrix. In the substitutional model, the N that replaces O in the TiO_2 lattice was taken to be bonded to three Ti atoms in the 96-atom supercell (a) so that the paramagnetic species is formally N^{2-}, whereas in the interstitial model N is added to the 96-atom supercell bonded to one or more O and thus is in a positive oxidation state as in NO^-, NO_2^- and/or NO_3^- (b)(see Figure 5). Figure 6 illustrates the DFT band structure of the N-doped TiO_2 and reports the calculated albeit still underestimated band gap energy of titania. The two bonding π states in Figure 6(b) for NO lie deep below the O 2p band but the two π^* still occupied states lie above (0.73 eV) the O 2p band and lie at higher energy than the 2p states of substitutional N (0.14 eV). A more interesting consequence of the picture of Figure 6 is that the two electrons left in the formation of an oxygen vacancy, which typically would form two Ti^{3+} color centers, may also be trapped by substitutional N_S and interstitial N_I yielding the azide species (N^{3-} denoted as N_S^-) and the hyponitrite species (NO^-). Another significant result deriving from the DFT calculations of Di Valentin and coworkers [48] is that N-doping leads to a substantively reduced energy of formation of V_Os (4.3 eV to 0.6 eV for anatase) with important consequences in the generation of *F*-type and Ti^{3+} color centers. Experimentally, which of the two types of N dopants predominates in the N-doped TiO_2 will depend on the experimental conditions, for example, nitrogen and oxygen concentrations, and calcination temperatures. What Figure 6 also implies is that moving from substitutional N to interstitial N is in fact an oxidative step, which according to DFT estimates is ca. 0.8 eV exothermic. Thus, there is a cost for the reverse, that is, interstitial N-doping is preferred when $TiO_{2-x}N_x$ systems are prepared in excess nitrogen and oxygen, whereas high-temperature calcination of N-doped systems, commonly done in most experiments, both substitutional N and formation of oxygen vacancies V_Os are likely the preferred occurrences.

The question on the blue-shift of the absorption edge of N-doped TiO_2 rutile single crystals contrasting the red-shifts in N-doped TiO_2 powders was also taken up in a DFT study by Yang and coworkers [49] using the plane-wave method. Results confirmed those of Di Valentin et al. [47] that some N 2p states lay above the O 2p valence band when N substitutes O in the TiO_2 lattice and when N is located at interstitial positions. However, *no band gap narrowing* was predicted by the calculations of Yang et al. [49]. When N substitutes Ti atoms in the rutile lattice, a band gap narrowing in the rutile crystal is apparently possible because the N dopant introduces some energy states (the N 2p states) into the bottom of the conduction band [49]. The authors rationalized this inference by the fact that removal of electrons from the supercell on replacing one Ti with a N atom leads to a reduction of the Coulomb repulsion and thus to a shift of the energy band edges, that is, the band gap energy is reduced by ca. 0.25 eV relative to the undoped rutile supercell whose estimated band gap energy was calculated to be 1.88 eV. This is reminescent of the assertion by Asahi et al. [4, 46] that N-doping TiO_2 causes band gap narrowing because the N 2p states mix with the O 2p states in the valence band, thereby widening the valence band and shrinking the band gap.

Substitutional N-doping can be stabilized by the presence of oxygen vacancies ($N_{S-}O + V_O$) under oxygen-poor experimental conditions, whereas under oxygen-rich conditions interstitial N species (N_I) become favored. The N-doped sample prepared by the sol-gel process of stoichiometry near $TiO_{1.907}N_{0.062}$, examined earlier by Di Valentin and coworkers [48], was re-examined more closely by Livraghi et al. [50] in a series of experiments and DFT calculations aimed at determining the fate of the doped specimen when irradiated at different wavelengths in the presence of adsorbates. The experiments asserted that N species were responsible for the absorption of visible-light radiation, and consequently for the visible-light activity, as well as for the photoinduced electron transfer from the solid to surface electron scavengers (adsorbates) such as molecular O_2. The UV-visible diffuse reflectance spectrum of the sample (see Figure 7) is nearly identical to the many reported DRS spectra of N-doped TiO_2 specimens prepared in a variety of ways. However, as we will see below, this spectral behavior is identical to the spectral behavior of so many other doped TiO_2 samples that have been doped with different types of dopants (e.g., transition metal ions, C, S, and others) and synthesized by different methods. Previous EPR work (Di Valentin et al. [48]) had identified two distinct N-related paramagnetic species in N-doped TiO_2, one of which was the molecular NO radical [51] located in closed pores within the crystals and thus had no influence on the electronic structure of the solid. No evidence of NH_x-type paramagnetic species was found as had been reported by Yates' group [31, 32]. Whatever the nature of the paramagnetic species, it was stable to washing and to calcination in air up to ca. 500 C. This was taken to mean that the nitrogen radical species, identified as $N_b^\bullet$ in Figure 8 interact strongly with the TiO_2 lattice. DFT calculations carried out on the 96-atom supercell involved two interstitial nitrogens ($N_I^\bullet$) or two substitutional nitrogen ($N_S^\bullet$) paramagnetic species plus an oxygen vacancy (V_O) located far away from these N-centers to avoid direct defect/impurity interactions. Note that removal of an O atom from the TiO_2 lattice leaves behind two electrons to form the *neutral F*center (V_O in the Kroger-Vink notation), or they may be trapped by neighboring Ti^{4+} species to give two Ti^{3+} color centers, which Henderson et al. [52] positioned at 0.8 eV below the bottom of the conduction band. Other studies indicated otherwise, although there are electron traps around this energy. Ti^{3+} color centers certainly do exist as demonstrated by EPR measurements [53, 54]. One of the consequences of the high number of V_Os under oxygen-poor conditions in N-doped

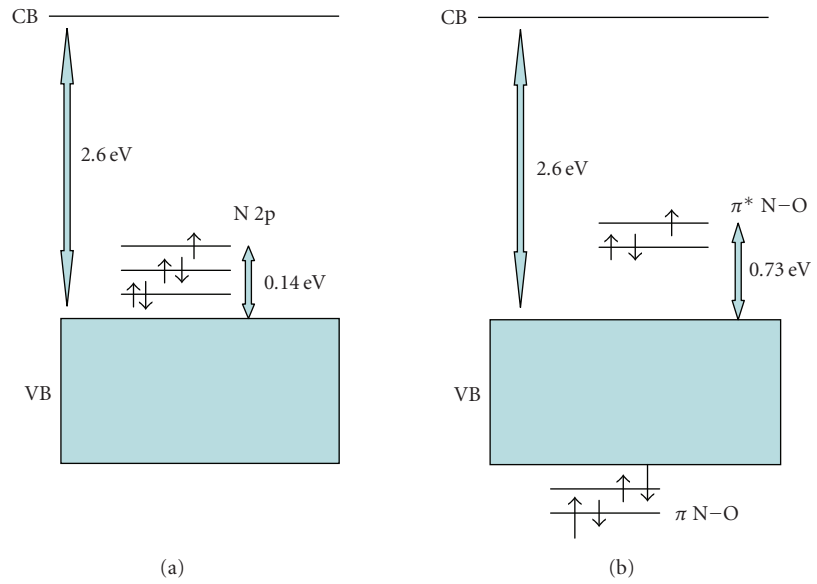

Figure 6: Electronic band structure for (a) substitutional and (b) interstitial N-doped anatase TiO_2 as given by PBE calculations at a low-symmetry k-point. In the former, the site contains the paramagnetic N^{2-} species making the site electrically neutral (replaced O^{2-}), whereas in the latter the site is occupied by the radical NO. The estimated band gap energy is also indicated. Reproduced with permission from [48]. Copyright (2005) American Chemical Society.

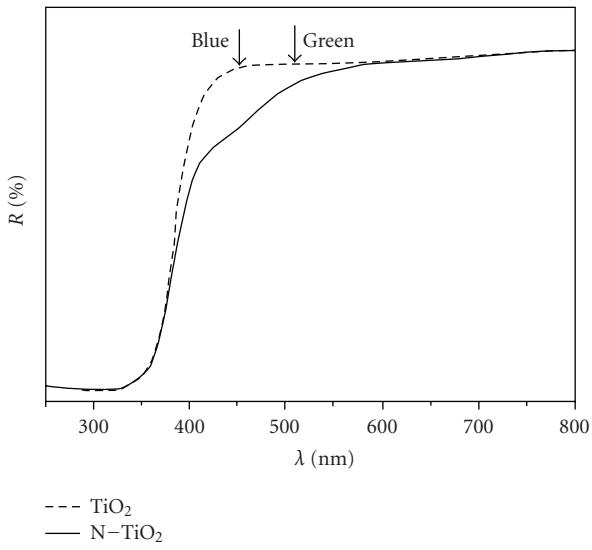

Figure 7: UV-visible diffuse reflectance spectra of undoped and N-doped TiO_2. Reproduced with permission from [50]. Copyright (2006) American Chemical Society.

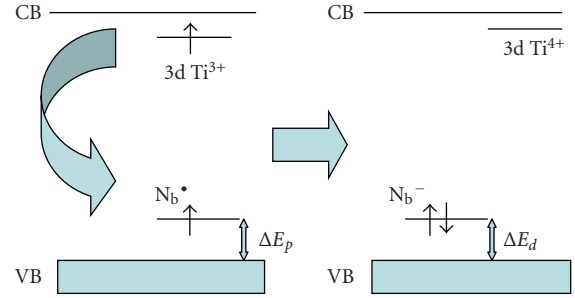

Figure 8: Electronic band structure changes from interactions between $N_b^{\bullet}$ ($N_S^{\bullet}$ or $N_I^{\bullet}$) and Ti^{3+} color centers. Reproduced with permission from [50]. Copyright (2006) American Chemical Society.

TiO_2 is the partial quenching of $N_b^{\bullet}$ paramagnetic species, which are transformed [48] into N_b^{-} through reduction by Ti^{3+} color centers (see Figure 8). The energetically favored reduction of $N_b^{\bullet}$ species may be the cause for the small energy cost in the formation of V_Os in N-doped TiO_2 (see above). The EPR peaks attributed to $N_b^{\bullet}$ centers disappeared on reduction of the sample (reaction (2)) whether by annealing in vacuo or by other means to then reappear on re-oxidation. Thus, the N-doped TiO_2 specimen (at least the one prepared by the sol-gel method) contained paramagnetic N related species in the bulk lattice ($N_b^{\bullet}$) and a number of diamagnetic species (N_b^{-}), the presence of which depended on the oxygen content in the metal-oxide sample. The EPR signal due to $N_b^{\bullet}$ increased on irradiating the doped sample at 437 nm in O_2(p_{O2} = 5 kPa). A new EPR line appeared that was attributed to $O_2^{-\bullet}$ radical anions (reactions (3) and (4)). These anions are apparently stabilized on two different surface Ti^{4+} species, which Livraghi et al. [50] claimed could be typical of N-doped TiO_2. Figure 9 illustrates the process embodied in the formation of the superoxide radical

$$N_b^{\bullet} + Ti^{3+} \longrightarrow N_b^{-} + Ti^{4+} \quad (2)$$

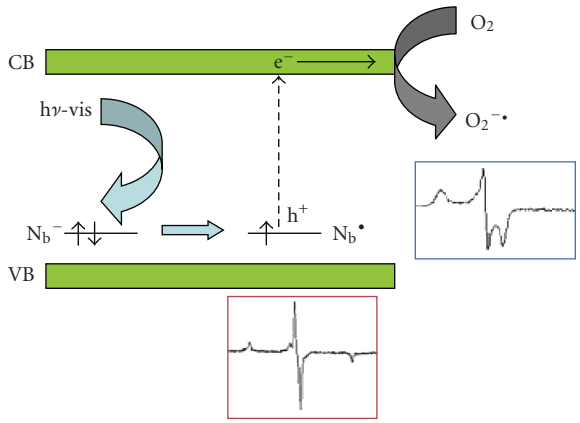

Figure 9: Sketch of the proposed mechanism for the processes induced by vis-light irradiation of the N-doped sample in O_2 atmosphere. Reproduced with permission from [50]. Copyright (2006) American Chemical Society.

anions

$$N_b^- + h\nu \longrightarrow N_b^\bullet + e^-_{surf} \quad (3)$$

$$e^-_{surf} + O_2 \longrightarrow O_2^{-\bullet}. \quad (4)$$

So far all the DFT-based calculations *have failed* to calculate experimentally commensurate band gap energies for undoped anatase and rutile TiO_2, and consequently for all anion-doped TiO_2 systems unless, as some have done, one resorts to the scissor operator. In a comprehensive theoretical investigation of substitutional anion doping in TiO_2, Wang and Lewis [55] explored the electronic properties of C-, N-, and S-doped TiO_2 materials using an *ab initio* tight-binding method (FIREBALL) based on density functional theory and a nonlocal pseudopotential scheme. The method uses confined atomic-like orbitals as the basis set, which led to a calculated direct band gap from Γ to Γ of 3.05 eV for rutile that accords with the experimental band gap of 3.06 eV [56]. The local density approximation (LDA) approach generally underestimates the experimental band gap for insulators and semiconductors; *ab initio* plane-wave calculations for TiO_2 also place the band gap at around 2.0 eV [57]. In their theoretical treatment, Wang and Lewis [55] compensated for the underestimation by the LDA approach. For anatase, the direct band gap from Γ to Γ of 3.26 eV accords with the experimentally observed 3.20 eV [58]—see Table 1. The upper valence bands are composed mainly of O 2p states, whereas the lower conduction bands consist primarily of unoccupied Ti 3d states.

In the computations of Wang and Lewis [55], two O atoms were replaced by one N because of the odd number of electrons in the N atom to yield an effective N-doping level of 0.52% in the low concentration case. The CB minimum remained unchanged. However, new states were introduced by N-doping just above the valence band edge of bulk TiO_2, as well as states that penetrated into the upper valence band of the bulk states. No significant energy shift (<0.05 eV) in the VB edge was seen in N-doped *rutile* TiO_2 at the high N content of 5.2%, contrary to the significant shift observed for the low N-doping level of 0.52% which gave a narrowed band gap of 2.55 eV. Density-of states (DOS) calculations thus inferred that low doping N levels greatly improve the visible-light photoactivity. No significant overlap occurred between the N 2p states and the O 2p states for the 0.52%N-doping level. Moreover, at the low N concentration the valence band edge was more localized compared to the high N-doping level in N-doped *rutile* TiO_2. Unlike N-doped *rutile* TiO_2, however, identical shifts of ca. 0.44 eV were obtained in N-doped *anatase* TiO_2 at both high and low doping levels resulting in a band gap of ca. 2.82 eV (440 nm). DOS calculations indicated significant overlap between the N 2p states and O 2p states for the 5.2% N-doping. By contrast, at the low N-doping level of 0.52% N, the states introduced by N were distinct, highly localized on the single dopant state, and there was no significant overlap. A result of this is that the high N-doping level in N-doped *anatase* TiO_2 would lead to greater visible-light photoactivity.

Table 1: Comparison of calculated band gaps of undoped rutile and anatase TiO_2 with experimental and calculated values reported by others (E_{BG} is the direct band gap). From Wang and Lewis [55].

Source	E_{BG} (rutile), eV	E_{BG} (anatase), eV
Wang and Lewis	3.05	3.26
Experiments	3.06 [56]	3.20 [58], 3.42 [59]
Other calcns	2.00 [57], 1.78 [60]	2.22 [60], 2.00 [46]

The brief discussion above points to a lack of consensus on whether or not there is *band gap narrowing* in doped TiO_2 materials based on DFT calculations. Some of the theoretical studies have deduced from these calculations that there is a *rigid shift of the valence band edge* to higher energies, thus narrowing the *intrinsic band gap* of TiO_2 as a consequence of doping. The discrepancies cannot be attributed to a simple semantic problem. Experimentally, anion-doping and cation-doping of TiO_2 do red-shift the *absorption edge* of TiO_2 in the doped samples, thus yielding potentially visible-light photoactive materials that might prove useful in several important applications of surface processes occurring on the TiO_2 surface. In the past, we have referred to the longest visible-light wavelength at which photoactivity is seen as the *red limit of photocatalysis*. We wish to emphasize, however, that what does change is the lowest photo-threshold (i.e., *extrinsic* absorption edge) of the actinic light that can activate TiO_2 by introducing dopants into the metal-oxide lattice. When a N-doped TiO_2 system is photoactivated by visible light absorption, it also generates electrons and holes, although the latter carriers will have a decreased oxidative power (lower redox potential) *vis-a-vis* holes photogenerated from pristine TiO_2 (see, e.g., Figure 3). The *intrinsic* absorption edge of the metal oxide itself is not changed by the doping. In other words, the valence and conduction bands are not affected by the doping, *at least* at low doping levels and weak interactions. But if they were to be affected through strong coupling interactions between the dopant states and the O 2p states of the VB of TiO_2, as some have surmised by DFT calculations, then we must face the inescapable conclusion that the material is no longer TiO_2, but is some titanium

oxynitride material (for N-doped TiO_2) that possesses entirely different properties, not least of which are new electronic structures of their respective valence and conduction bands. In this regard, a recent study by Kim and coworkers [61] has demonstrated that a solid solution prepared from ZnO and ZnS, which could be referred to as S-doped $ZnO(ZnO_xS_{1-x})$ displays an absorption edge in the visible spectral region at 2.4 eV *vis-à-vis* the absorption edges of both ZnO (3.1 eV) and ZnS (3.5 eV). The XRD patterns indicated a new material, namely a zincoxysulfide phase, whose band gap is 2.4 eV, much narrower than either of the band gaps of the two initial substrates owing to strong coupling of the S 2p states with the O 2p states in the valence band of the *new* material. Note that in all the doped TiO_2 systems, XRD patterns showed that the doped TiO_2 retained the anatase (or rutile) structure; no new phase or new material could be ascertained.

4. OPTICAL PROPERTIES OF N-DOPED TiO_2

An examination of the optical properties of doped TiO_2 provides evidence based on the photobleaching phenomenon that the absorption bands observed in the visible spectral region for (any) doped TiO_2 material can be bleached. That is, the species that give rise to or that are responsible for the absorption bands in the visible spectral region of doped TiO_2 can be destroyed by irradiating with visible-light wavelengths corresponding to the absorption bands in the visible spectral region, or by a heat treatment. Under these conditions, it is important to recognize that neither the *intrinsic* VB nor the *intrinsic* CB can be destroyed.

Optical properties of doped TiO_2 specimens can be discussed in terms of difference diffuse reflectance spectra (ΔDRS) calculated from the DRS of various doped TiO_2 samples absorbing in the visible region [$\rho_{abs}(h\nu)$] and undoped TiO_2 samples that do not absorb in the visible spectral region [$\rho_{non\text{-}abs}(h\nu)$]. The latter is typically the DRS of a nominally clean TiO_2 sample or the DRS of the doped sample *prior* to any treatment that might induce visible-light absorption [62]. Where the transmittance spectrum of a thick sample is 0, the change in reflectance $\Delta\rho(h\nu)$, that is, $[\rho_{non\text{-}abs}(h\nu) - \rho_{abs}(h\nu)]$ is then identical to the change in absorbance $\Delta A(h\nu)$. Moreover, where optical properties of doped specimens are characterized by absorption spectra $A(h\nu)$, the difference absorption spectra $\Delta A(h\nu)$ can be calculated in a manner similar to the difference DRS spectra, $\Delta\rho(h\nu)$. Usage of difference diffuse reflectance and/or difference absorption spectra provides a means for numerical analysis of the optical characteristics of the samples. The analysis typically involves (i) the characterization of each absorption spectrum by the position of the spectral maximum ($h\nu_{max}$), the intensity of this maximum ($\Delta\rho_{max}, \Delta A_{max}$), and the spectral bandwidth at half-maximum amplitude, (ii) the comparison of the spectra of different samples after normalization by the $\Delta\rho_{max}/\Delta A_{max}$ factor, and (iii) the analysis of the shape of the absorption spectra to display the spectra as a sum of individual absorption bands.

Resulting absorption spectra of various nondoped TiO_2 specimens displaying maximal absorption around 3.0 eV and

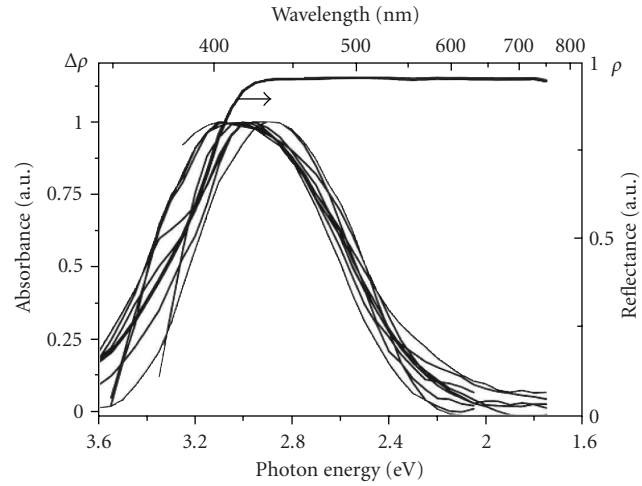

Figure 10: Absorption spectra of various anion-doped TiO_2 specimens before averaging (see text) and the diffuse reflectance spectrum (DRS) of Degussa P25 TiO_2.

shown in Figure 10 are those of (i) mechanochemically activated N-doped TiO_2 [17], (ii) N-doped oxygen-deficient TiO_2 [13], (iii) N,F-codoped TiO_2 sample prepared by a spray pyrolytic method [63], (iv) N-doped *anatase* TiO_2 specimen prepared by a solvothermal process [37], (v) N-doped *rutile* TiO_2 sample also prepared by a solvothermal process [37], (vi) *yellow* N-doped TiO_2 specimen synthesized in short time at ambient temperatures using a nanoscale exclusive direct nitridation of TiO_2 nanocolloids with alkyl ammonium compounds [19, 20], (vii, viii) N-doped TiO_2 samples prepared by evaporation of the sol-gel with N-doping carried out under a stream of ammonia gas at different temperatures [40], and (ix) N-doped TiO_2 prepared via sol-gel by mixing a solution of titanium (IV) isopropoxide in isopropyl alcohol in the presence of an NH_4Cl solution [50].

Temperature and time of calcination are frequently reported as factors that affect the shape of the absorption spectra. For instance, an increase of temperature from 247 C to 347 C for 2 hrs [64], or prolonging the time of calcination from 5 min to 30 min at 400 C [40], decreased the absorption in the range $h\nu < 2.0$ eV, such that the absorption spectra then adopted a narrower shape. As an example, the broad absorption spectrum of the *orange* N-doped TiO_2 specimen, prepared in nearly the same manner as the *yellow* N-doped TiO_2 sample by Gole et al. [19, 20], showed a shoulder on the high-energy side at ca. 2.5 eV (see Figure 12, curve 3 below). Surprisingly, Figure 10 demonstrates a strong similarity between selected spectra in the visible region at energies $h\nu < 3.0$ eV, and noticeable differences in the range of *intrinsic* absorption at $h\nu > 3.0$ eV. Such differences are not surprising since the samples differed in phase composition (see, e.g., [37]) and sample thickness. Moreover, some workers often choose any available sample, for example, Degussa P25 TiO_2, as the nonabsorbing specimen in the visible spectral region, rather than a specimen prepared in an otherwise identical fashion as the doped samples. Spectral similarities in Figure 10 afford averaging the spectra to obtain the mean

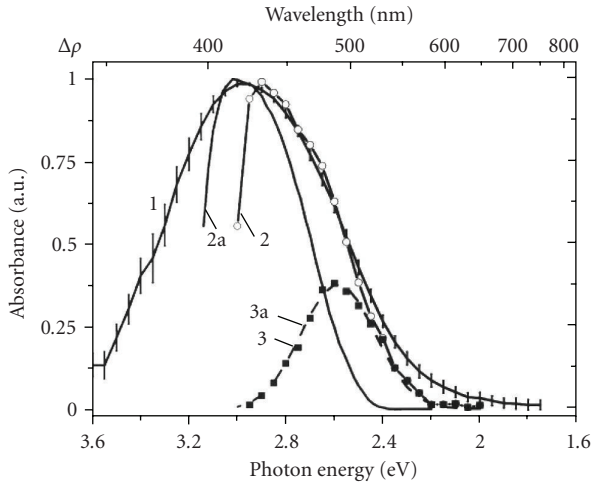

Figure 11: Average absorption spectrum of visible-light-active N-doped TiO_2 specimens (curve 1); difference absorption spectra of N-doped rutile crystal (curve 2) and of the color centers in the yellow anatase TiO_2 crystal (curve 2a). Curve 3 (solid squares) depicts the difference between curves 2 and 2a; curve 3a (line) is the Gaussian fit of curve 3 (see text for more details).

spectrum of visible-light-active N-doped TiO_2 samples illustrated in Figure 11 (curve 1; standard error of the mean spectrum was less than 2.3% at $h\nu < 3.0$ eV). Figure 11 also displays the absorption spectrum of the N-doped TiO_2 rutile crystal prepared by an NH_3 treatment at 597 C (curve 2) [21] and the absorption spectrum of the anatase crystal (curve 2a) reported by Sekiya and coworkers [65, 66].

The difference in spectra 2 and 2a in the region $h\nu > 3.0$ eV originates from the difference in the phase composition of the TiO_2, whereas the difference between curves 2a and 2 at $h\nu < 3.0$ eV exhibits a single absorption band with $h\nu_{max} = 2.6$ eV, half-width of 0.35 eV and a near-Gaussian shape, that is, the band is very similar to the 2.55-eV AB2 band reported earlier by Kuznetsov and Serpone [62]. Sekiya and coworkers [65, 66] attributed the 3.0-eV band in the spectrum of anatase to oxygen vacancies that can trap electrons to yield *F*-type centers [66]. It should be emphasized that the AB1 absorption band with $h\nu_{max}$ at 3.0 eV can be obtained in a variety of ways: (i) by annealing the *as-grown* crystals under an oxygen atmosphere at T > 374 C [65, 66], and (ii) by annealing *colorless* crystals by subjecting them first to a reductive H_2 atmosphere at 647 C and then to an O_2 atmosphere at 497 C [66]. In both cases, only prolonged (ca. 60 hrs) annealing of the crystals at 797 C in an O_2 atmosphere (not inert or nitrogen atmosphere) transformed the yellow crystals displaying a band at 3.0 eV to a colorless state [66]. The origin of oxygen vacancies is associated with an uncontrolled reduction of TiO_2 assisted by impurities introduced into the crystal during its growth [65]. Absorption of N-doped rutile crystals in the visible spectral region is only partially associated with reduction of the TiO_2 bulk lattice [32]. According to Yates and coworkers [31–33] the red-shift in the photochemical threshold from 3.0 eV to 2.4 eV originates from the N dopant located in an interstitial site and probably bonded to hydrogen. This suggestion contrasts the interpretation given by Sekiya and coworkers for the spectral features in the visible region [65, 66], by Di Valentin et al. from their EPR study [48], and with our assignments of absorption bands in the visible spectral region of various titania/polymer compositions [62].

The remarkable similarities in the absorption spectra of doped TiO_2 systems are displayed in Figure 12 as averaged spectra. Curve 1 depicts the average spectrum obtained from the absorption spectra (see [62] for details) of (i) Cr-implanted TiO_2, (ii) Ce-doped TiO_2, (iii) mechanochemically activated N-doped TiO_2, (iv) N-doped oxygen-deficient TiO_2, and (v) from $Sr_{0.95}La_{0.05}TiO_{3+\delta}$ treated with HNO_3 acid. Curve 2 represents the average spectrum obtained from the difference DRS's (absorption spectra) of various anion-doped titania specimens: (i) N,F-codoped TiO_2, (ii) N-doped anatase TiO_2, (iii) N-doped rutile TiO_2, and (iv) yellow nitrided $TiO_{2-x}N_x$ nanocolloids. Curve 3 illustrates the averaged spectra of cation-doped TiO_2, namely (i) Fe-doped TiO_2 nano-powders prepared by oxidative pyrolysis of organometallic precursors in an induction thermal plasma reactor, (ii) zinc-ferritedoped titania ($TiO_2/ZnFe_2O_4$) synthesized by sol-gel methods followed by calcinations at various temperatures, and (iii) the orange N-doped TiO_2 sample prepared by a procedure otherwise identical to that of yellow N-doped TiO_2 but with the former consisting of partially agglomerated nanocolloids (i.e., larger $TiO_{2-x}N_x$ clusters). Note the remarkable overlap of the relatively narrow average spectra 1 and 2 in Figure 12, which illustrates convincingly the independence of the spectra on the method of photocatalyst preparation. Such overlap features can only result from electronic and spectral features of color centers/defects in TiO_2. Comparison of the broader mean spectrum 3 in Figure 12 with the narrower spectra 1 and 2 shows that broadening of the absorption spectrum of TiO_2 photocatalysts originates from the long-wavelength AB2 absorption band at 2.55 eV [62].

The remarkable coincidence of the absorption bands in the visible spectra of reduced TiO_2 with those of visible-light-active TiO_2s infers that processes involved in the preparation of visible-light-active TiO_2 specimens (irrespective of the method) likely implicate a stage of TiO_2 reduction. Indeed, most of the syntheses included a heating stage at various temperatures. For example, the 3.0 eV absorption band of anatase crystals attributed to oxygen vacancies results from the removal of impurities introduced during the crystal growth at ca. 300 C [65]. Related to this, the visible-light absorption of metal-ion-implanted TiO_2s was observed only after the samples had been calcined in the temperature range 450–550 C [2]. Accordingly, the absorption features displayed by TiO_2 specimens in the visible spectral region likely originate from the formation of color centers by reduction of TiO_2 after some form of heat treatment or some photostimulated process. Kuznetsov and Serpone [62] concluded that the visible absorption spectra of anion-doped (or otherwise) TiO_2 originated from color centers, and not from the narrowing of the intrinsic band gap of TiO_2 (E_{bg} = 3.2 eV; anatase), as originally proposed by Asahi et al. [4, 46] through mixing of oxygen and dopant states. True narrowing

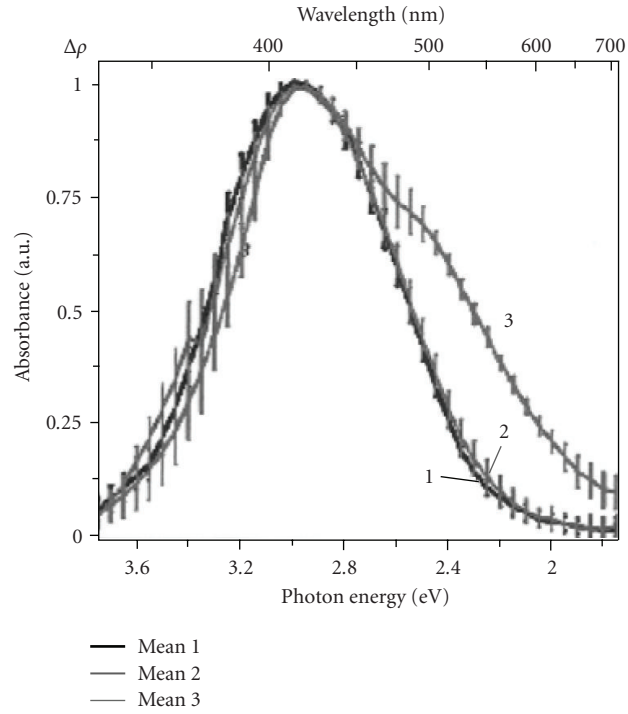

Figure 12: Average absorption spectra ($\Delta\rho$) of various titania systems. See text for details of the origins of these spectra. Reproduced with permission from [62]. Copyright (2006) American Chemical Society.

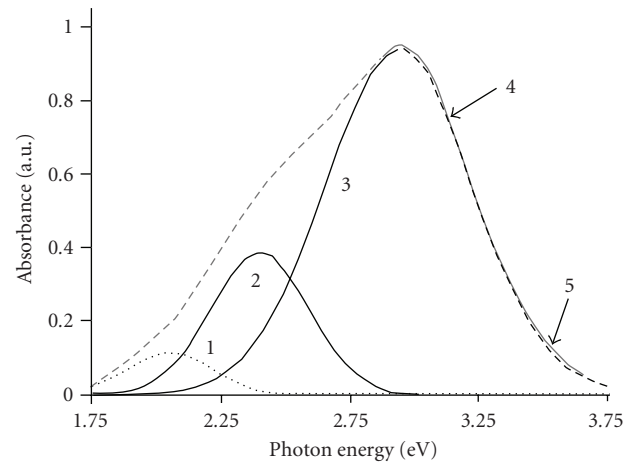

Figure 13: Deconvolution of spectrum 3 of Figure 12 (curve 5 herein). Band 4 represents the convolution sum of curves 1, 2, and 3. Reproduced with permission from [67]. Copyright (2006) American Chemical Society.

of the intrinsic band gap of a metal oxide such as TiO_2 would necessitate heavy anion or cation doping at high concentrations of dopants. In such case, however, one must question whether the metal oxide retains its original integrity. We think not as exemplified from the recent reported case of the zincoxysulfide [61].

The next question regards the nature of these color centers. Loss of an O atom in a metal oxide (reaction (5)), leaves behind an electron pair that is trapped in the V_O cavity (reaction (6)) giving rise to an F center; an F^+ center is equivalent to a single electron trapped in the oxygen vacancy, $V_O^{\bullet}$ (reaction (7); Kroger-Vink notation). The electron-pair deficient oxygen vacancy, $V_O^{\bullet\bullet}$, also known as an anion vacancy, V_A, is a doubly charged F^{++} center (reaction (5)). Thus, color centers associated with oxygen vacancies imply F-type centers in TiO_2 and other metal oxides. In addition, electrons can also be trapped by Ti^{4+} ions in regular lattice sites ($Ti^{4+}{}_{reg}$) adjacent to V_O or in interstitial lattice sites ($Ti^{4+}{}_{int}$) to give $Ti^{3+}{}_{reg}$ and $Ti^{3+}{}_{int}$ color centers, respectively (reactions (8a)); F-type centers can also generate Ti^{3+} color centers through charge transfer (reaction (8b)),

$$Ti^{4+}\text{–}O^{2-}\text{–}Ti^{4+} \longrightarrow Ti^{4+} - \square - Ti^{4+} + V_O^{\bullet\bullet}(F^{++}) + 2e^- \tag{5}$$

$$V_O^{\bullet\bullet} + 2e^- \longrightarrow V_O(F) \tag{6}$$

$$V_O^{\bullet\bullet} + 2e^- \longrightarrow V_O^{\bullet}(F^+) \tag{7}$$

$$e^- + Ti^{4+}{}_{reg}\{Ti^{4+}{}_{int}\} \longrightarrow Ti^{3+}{}_{reg}\{Ti^{3+}{}_{int}\} \tag{8a}$$

$$F(\text{or } F^+) + Ti^{4+}{}_{reg}\{Ti^{4+}{}_{int}\} \longrightarrow Ti^{3+}{}_{reg}\{Ti^{3+}{}_{int}\} + F^+(\text{or } F^{++}). \tag{8b}$$

Spectrum 3 of Figure 12 consists of three overlapping bands depicted in Figure 13 [67], one of which is centered at 2.1 eV (590 nm; band 1), another at ca. 2.40 eV (517 nm; band 2), and band 3 occurs around 2.93 eV (413 nm) in accord with band positions reported earlier by Kuznetsov and Serpone [62] for reduction of TiO_2 in polymeric media. The congruence of the bands in the absorption spectra of such disparate TiO_2 systems is remarkable when considering the large variations in the experimental conditions. This lends credence to the notion that the absorption bands likely share the same origins, namely electron transitions involving F-type centers and/or d-d transitions in Ti^{3+} color centers. Evidence for both has appeared in the literature (see references in [67]).

Using the embedded-cluster numerical discrete variational method, Chen et al. [68] estimated the band gap energy of rutile TiO_2 as 3.05 eV in good agreement with the experimental 3.0 eV for this polymorph. Calculations of energy levels of F-type centers gave energies for the F, F^+ and F^{2+} centers, respectively, of 0.87 eV, 1.78 eV and 0.20 eV below the bottom level of the CB band (see Figure 14). The band at 760 nm (1.61 eV) was ascribed to the electron transition $F^+ \rightarrow$ CB of TiO_2.

Photoinduced detrapping of electrons from the F center to the conduction band followed by retrapping by the shallow F^{2+} centers can increase the number of F^+ centers. The deconvoluted bands 3 and 2 of Figure 13 at 2.9–3.0 eV (428–413 nm) and 2.4–2.6 eV (ca. 517–477 nm), respectively, have been attributed [67] to Jahn-Teller split $^2T_2 \rightarrow {}^2E$ transitions of Ti^{3+} centers. Existence of these centers has been confirmed by EPR examination of N-doped TiO_2 specimens calcined at various temperatures [40, 69]. Band 1 at 1.7–2.1 eV (729–590 nm) is likely due to the transition $F^+ \rightarrow F^{+*}$,

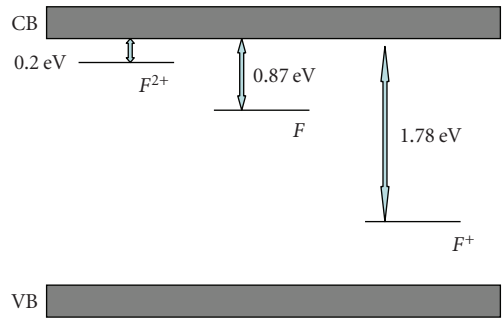

Figure 14

though the transition $F^+ \rightarrow$CB is not precluded. The transition $S_o(F) \rightarrow S_1(F^*)$or $S_o(F) \rightarrow$CB of the F center likely occur at much lower energies (in the infrared). Rigorous systematic studies are needed to ascertain such assignments in anion- and cation-doped TiO_2 specimens examined by diffuse reflectance spectroscopy; additional EPR and photoconductivity studies should aid in such task.

5. IS THE (*INTRINSIC*) BAND GAP OF TiO_2 NARROWED IN N-DOPED TiO_2?

Taken literally, band gap narrowing in doped TiO_2 materials means that the *intrinsic* band gap energy of TiO_2 decreases in the presence of dopants. We re-emphasize that what does change is the energy photothreshold for activating doped titania specimens to carry out surface photoinduced redox processes. A better term to refer to the red-shift of the absorption edge might be (i) the *red-limit of TiO_2 photocatalysis*, used in the past to refer to redox processes occurring in the visible spectral region or (ii) the *extrinsic band gap(s)* of doped TiO_2 *versus* the term *intrinsic band gap* which for anatase is 3.2 eV and for rutile is 3.0 eV; the latter refer to pristine undoped titania. The term *band gap narrowing* used by Asahi et al. [4, 46] and others meant a rigid upward shift of the valence band edge toward the conduction band of TiO_2. If the red-shift of the absorption edge were truly due to this rigid shift, then irradiation into the visible spectral bands of Figure 13 should cause no bleaching of the absorption bands. However, if the absorption features are due to the existence of color centers (F-type and/or Ti^{3+}), then bleaching of the spectral features should occur as observed in our recent studies on TiO_2/polymer compositions [70] and on a N-doped TiO_2 system [71] that we now examine briefly.

The photocoloration of TiO_2/polymers compositions and the photobleaching of color centers (see Figure 15) at various irradiation wavelengths (UV to near-IR region) were examined to probe the photoactivation of color centers on irradiating into the absorption bands at 2.90 eV (427 nm; AB1), 2.55 eV (486 nm; AB2) and 2.05 eV (604 nm; AB3). Such exercise should lead to two principal types of photostimulated absorbance changes: (i) increase in absorbance or (ii) decrease in absorbance. The decrease in absorbance (ii) is a direct experimental manifestation of the photobleaching phenomenon of colored TiO_2/polymer

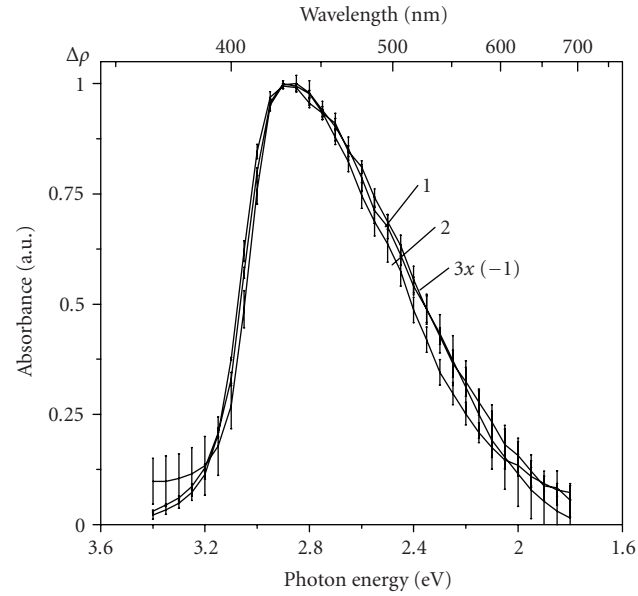

Figure 15: Averaged absorption spectra (1, 2) of various TiO_2/polymer compositions normalized by $\Delta\rho_{max}$ and averaged bleaching spectrum (3) of the TiO_2/[P(VDF-HFP)] composition irradiated at different wavelengths. Reproduced with permission from [70]. Copyright (2007) American Chemical Society.

compositions and would clearly demonstrate the presence and photoinduced disappearance/destruction of color centers in such TiO_2/polymers systems. The average spectrum of the bleaching of the colored TiO_2/[P(VDF-HFP)] composition {P(VDF-HFP) is poly(vinylidene fluoride/co-hexafluoropropylene polymer)} is depicted as curve 3 in Figure 15 and is compared to the average heat-induced absorption spectrum (curve 1) and photoinduced absorption spectrum (curve 2) of several other TiO_2/polymer compositions [70]. These observations confirm an earlier proposal [62] that absorption of light by various TiO_2 systems in the visible region originates *only* from color centers and *not* from a narrowing of the band gap of pristine TiO_2. Results also indicate that photobleaching of colored TiO_2/polymer compositions originates both from *intrinsic* absorption of light ($h\nu > 3.2$ eV, anatase) by TiO_2 and from (*extrinsic*) absorption of light by the color centers at wavelengths corresponding to their absorption spectral bands in the visible region. These bands are also active in the photodestruction of the color centers. Spectrum 3 in Figure 15 corresponds to the nearly complete discoloration of the compositions under irradiation mostly in the visible region. Hence, the total overlap of the absorption and bleaching spectra of Figure 15 *demonstrate unambiguously* that the *same* color centers are formed during the treatment that induced the absorption, and that they are subsequently destroyed on irradiation during the photobleaching process. These data conclusively negate any inference of broadening of the valence band of TiO_2 to account for the red-shifts of the absorption edges in doped visible-light-active TiO_2 systems. The VB and CB bands *can neither* be photodestroyed *nor* phototransformed,

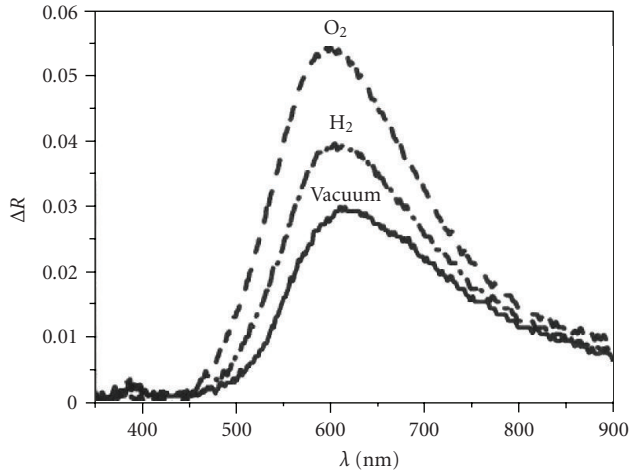

Figure 16: Absorption spectra of photoinduced color centers in N-doped TiO_2 obtained after pre-irradiation at 546 nm in vacuum, in the presence of O_2 and H_2. Reproduced with permission from [71]. Copyright (2007) American Chemical Society.

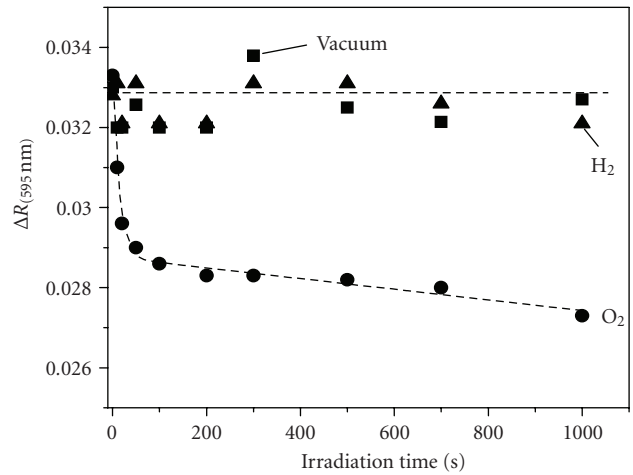

Figure 17: Kinetics of photobleaching (recorded at $\lambda = 595$ nm) of photoinduced color centers on irradiation of $TiO_{2-x}N_x$ at $\lambda > 610$ nm in vacuum, in the presence of oxygen and in the presence of hydrogen. Reproduced with permission from [71]. Copyright (2007) American Chemical Society.

contrary to the color centers. An additional study [71] examined the effect of molecular oxygen and hydrogen on the photostimulated formation of defects (color centers) on irradiation of $TiO_{2-x}N_x$ with visible light (546 nm). Results are displayed in Figure 16 as ΔR versus λ; note that ΔR and $\Delta\rho$ have the same meaning, namely absorbance. A similar behavior was observed on irradiating at 436 nm and 578 nm. The influence of hydrogen on photocoloration on irradiation at 546 nm is nearly the same as on UV irradiation, in that the number of photoinduced defects increased, contrary to when O_2 is present for which the photoadsorption of O_2 is the exact opposite to that seen under UV irradiation. The ultimate level of photocoloration (increase in absorption) in the presence of O_2 is considerably greater under 546-nm irradiation relative to the level in vacuum and relative to what is observed under UV irradiation. This inferred the mechanism of photoexcitation and surface photoreaction occurring under visible-light excitation of $TiO_{2-x}N_x$ in the presence of O_2 is different from the mechanism of UV-induced processes. Photobleaching of photoinduced color centers by red light at $\lambda > 610$ nm in vacuum and in the presence of oxygen and hydrogen is illustrated in Figure 17. No significant changes in absorption of photoinduced color centers occur during photoexcitation in vacuum and in the presence of H_2. However, the presence of O_2 causes significant photo-bleaching (negative absorbance) of the UV-induced defects, a typical behavior of electron-type color centers (i.e., *F*-type and Ti^{3+} centers).

6. CONCLUDING REMARKS

In this survey, we have attempted to expose and explore some of the root causes that have had such impact and so changed the field of Heterogeneous Photocatalysis involving the next generation of TiO_2 photocatalysts. Preparative methods and some characteristic features of N-doped TiO_2s have been described briefly. At variance are the experimental results and interpretations of X-ray photoelectron spectra with regard to assignments of binding energy peaks. Relative to pristine nominally clean TiO_2, whose absorption edges are 3.2 eV (anatase) and 3.0 eV (rutile), N-doped TiO_2 specimens display red-shifted absorption edges into the visible spectral region. Several workers have surmised that the (*intrinsic*) *band gap* of TiO_2 is narrowed by the coupling of dopant energy states with the O 2p states in the VB band, an inference based on DFT computations of band gap energies, which are severely underestimated owing to the inherent faulty local density approximation (LDA). Using similar DFT calculations, others proposed that the red-shifted absorption edges originate from the presence of intragap dopant states above the upper level of the VB band. Analyses of spectral features in the visible region, however, inferred a common origin for the doped TiO_2 as deduced from the strong similarities of absorption features of a large number of TiO_2 specimens, regardless of the preparative methods employed and the nature of the dopants. This next generation of TiO_2 photocatalysts should enhance process engineering photoefficiencies, in some cases, since doped titania absorbs a greater quantity of sunlight radiation. The fundamental science that underscores Heterogeneous Photocatalysis with this new generation of photocatalysts is a rich playing field that is ripe for further exploration, limited only by one's imagination, creativity and resourcefulness.

REFERENCES

[1] D. Lawless, *Photophysical studies on materials of interest to heterogeneous photocatalysis and to imaging science: CdS quantum dots, doped and undoped ultrasmall semiconductor TiO_2 particles, and silver halides*, Ph.D. thesis, Concordia University, Montreal, Canada, 1993.

[2] M. Anpo and M. Takeuchi, "The design and development of highly reactive titanium oxide photocatalysts operating under visible light irradiation," *Journal of Catalysis*, vol. 216, no. 1-2, pp. 505–516, 2003.

[3] S. Sato, "Photocatalytic activity of nitrogen oxide (No_x)-doped titanium dioxide in the visible light region," *Chemical Physics Letters*, vol. 123, pp. 126–128, 1986.

[4] R. Asahi, T. Morikawa, T. Ohwaki, K. Aoki, and Y. Taga, "Visible-light photocatalysis in nitrogen-doped titanium oxides," *Science*, vol. 293, pp. 269–275, 2001.

[5] T. Morikawa, R. Asahi, T. Ohwaki, K. Aoki, and Y. Taga, "Band-gap narrowing of titanium dioxide by nitrogen doping," *Japanese Journal of Applied Physics, Part 2: Letters*, vol. 40, no. 6 A, pp. L561–L563, 2001.

[6] X. Chen and S. S. Mao, "Titanium dioxide nanomaterials: synthesis, properties, modifications and applications," *Chemical Reviews*, vol. 107, no. 7, pp. 2891–2959, 2007.

[7] X. Chen, Y. Lou, S. Dayal, et al., "Doped semiconductor nanomaterials," *Journal of Nanoscience and Nanotechnology*, vol. 5, no. 9, pp. 1408–1420, 2005.

[8] N. Serpone, A. V. Emeline, V. N. Kuznetsov, and V. K. Ryabchuk, "Second generation visible-light-active photocatalysts: preparation, optical properties and consequences of dopants on the band gap energy of TiO_2," in *Environmentally Benign Catalysts—Applications of Titanium Oxide-Based Photocatalysts*, M. Anpo and P. V. Kamat, Eds., Springer, New York, NY, USA, 2007.

[9] H. M. Yates, M. G. Nolan, D. W. Sheel, and M. E. Pemble, "The role of nitrogen doping on the development of visible light-induced photocatalytic activity in thin TiO_2 films grown on glass by chemical vapour deposition," *Journal of Photochemistry and Photobiology A: Chemistry*, vol. 179, no. 1-2, pp. 213–223, 2006.

[10] H. Noda, K. Oikawa, T. Ogata, K. Matsuki, and H. Kamata, "Preparation of titanium(IV) oxides and its characterization," *Bulletin of the Chemical Society of Japan*, pp. 1084–1090, 1986.

[11] N. C. Saha and H. G. Tompkins, "Titanium nitride oxidation chemistry: an x-ray photoelectron spectroscopy study," *Journal of Applied Physics*, vol. 72, pp. 3072–3079, 1992.

[12] D. H. Lee, Y. S. Cho, W. I. Yi, T. S. Kim, J. K. Lee, and H. J. Jung, "Metalorganic chemical vapor deposition of TiO_2: N anatase thin film on Si substrate," *Applied physics letters*, vol. 66, pp. 815–816, 1995.

[13] T. Ihara, M. Miyoshi, Y. Iriyama, O. Matsumoto, and S. Sugihara, "Visible-light-active titanium oxide photocatalyst realized by an oxygen-deficient structure and by nitrogen doping," *Applied Catalysis B: Environmental*, vol. 42, no. 4, pp. 403–409, 2003.

[14] H. Irie, Y. Watanabe, and K. Hashimoto, "Nitrogen-concentration dependence on photocatalytic activity of $Tio_{2-x}N_x$ powders," *Journal of Physical Chemistry B*, vol. 107, no. 23, pp. 5483–5486, 2003.

[15] T. Lindgren, J. M. Mwabora, E. Avandaño, et al., "Photoelectrochemical and optical properties of nitrogen doped titanium dioxide films prepared by reactive DC magnetron sputtering," *Journal of Physical Chemistry B*, vol. 107, no. 24, pp. 5709–5716, 2003.

[16] S. Sakthivel and H. Kisch, "Photocatalytic and photoelectrochemical properties of nitrogen-doped titanium dioxide," *ChemPhysChem*, vol. 4, no. 5, pp. 487–490, 2003.

[17] S. Yin, H. Yamaki, M. Komatsu, et al., "Preparation of nitrogen-doped titania with high visible light induced photocatalytic activity by mechanochemical reaction of titania and hexamethylenetetramine," *Journal of Materials Chemistry*, vol. 13, no. 12, pp. 2996–3001, 2003.

[18] M.-C. Yang, T.-S. Yang, and M.-S. Wong, "Nitrogen-doped titanium oxide films as visible light photocatalyst by vapor deposition," *Thin Solid Films*, vol. 469–470, pp. 1–5, 2004.

[19] C. Burda, Y. Lou, X. Chen, A. C. S. Samia, J. Stout, and J. L. Gole, "Enhanced nitrogen doping in TiO_2 nanoparticles," *Nano Letters*, vol. 3, no. 8, pp. 1049–1051, 2003.

[20] J. L. Gole, J. D. Stout, C. Burda, Y. Lou, and X. Chen, "Highly efficient formation of visible light tunable $Tio_{2-x}N_x$ photocatalysts and their transformation at the nanoscale," *Journal of Physical Chemistry B*, vol. 108, no. 4, pp. 1230–1240, 2004.

[21] X. Chen and C. Burda, "Photoelectron spectroscopic investigation of nitrogen-doped titania nanoparticles," *Journal of Physical Chemistry B*, vol. 108, no. 40, pp. 15446–15449, 2004.

[22] S. M. Prokes, J. L. Gole, X. Chen, C. Burda, and W. E. Carlos, "Defect-related optical behavior in surface-modified TiO_2 nanostructures," *Advanced Functional Materials*, vol. 15, no. 1, pp. 161–167, 2005.

[23] X. Chen, Y. Low, A. C. S. Samia, C. Burda, and J. L. Gole, "Formation of oxynitride as the photocatalytic enhancing site in nitrogen-doped titania nanocatalysts: comparison to a commercial nanopowder," *Advanced Functional Materials*, vol. 15, no. 1, pp. 41–49, 2005.

[24] C. S. Gopinath, "Comment on "photoelectron spectroscopic investigation of nitrogen-doped titania nanoparticles"," *Journal of Physical Chemistry B*, vol. 110, no. 13, pp. 7079–7080, 2006.

[25] S. Sato, R. Nakamura, and S. Abe, "Visible-light sensitization of TiO_2 photocatalysts by wet-method N doping," *Applied Catalysis A: General*, vol. 284, no. 1-2, pp. 131–137, 2005.

[26] E. György, A. Pérez del Pino, P. Serra, and J. L. Morenza, "Depth profiling characterisation of the surface layer obtained by pulsed Nd:YAG laser irradiation of titanium in nitrogen," *Surface and Coatings Technology*, vol. 173, no. 2-3, pp. 265–270, 2003.

[27] C. Burda and J. Gole, "Reply to comment on photoelectron spectroscopic investigation of nitrogen-doped titania nanoparticles," *Journal of Physical Chemistry B*, vol. 110, no. 13, pp. 7081–7082, 2006.

[28] H. Irie, Y. Watanabe, and K. Hashimoto, "Nitrogen-concentration dependence on photocatalytic activity of $TiO_{2-x}N_x$ powders," *Journal of Physical Chemistry B*, vol. 107, no. 23, pp. 5483–5486, 2003.

[29] R. Nakamura, T. Tanaka, and Y. Nakato, "Mechanism for visible light responses in anodic photocurrents at N-doped TiO_2 film electrodes," *Journal of Physical Chemistry B*, vol. 108, no. 30, pp. 10617–10620, 2004.

[30] T. Ma, M. Akiyama, E. Abe, and I. Imai, "High-efficiency dye-sensitized solar cell based on a nitrogen-doped nanostructured titania electrode," *Nano Letters*, vol. 5, no. 12, pp. 2543–2547, 2005.

[31] O. Diwald, T. L. Thompson, E. G. Goralski, S. D. Walck, and J. T. Yates Jr., "The effect of nitrogen ion implantation on the photoactivity of TiO_2 rutile single crystals," *Journal of Physical Chemistry B*, vol. 108, no. 1, pp. 52–57, 2004.

[32] O. Diwald, T. L. Thompson, T. Zubkov, Ed. G. Goralski, S. D. Walck, and J. T. Yates Jr., "Photochemical activity of nitrogen-doped rutile $TiO_2(110)$ in visible light," *Journal of Physical Chemistry B*, vol. 108, no. 19, pp. 6004–6008, 2004.

[33] T. L. Thompson and J. T. Yates Jr., "TiO_2-based photocatalysis: surface defects, oxygen and charge transfer," *Topics in Catalysis*, vol. 35, no. 3-4, pp. 197–210, 2005.

[34] P. Frach, D. Glöß, M. Vergöhl, F. Neumann, and K. Hund-Rinke, "Photocatalytic properties of titanium dioxide films prepared by reactive pulse magnetron sputtering," in *Proceeding of the 4th International Workshop on the Utilization and Commercialisation of Photocatalytic Systems (EJIPAC '04)*, Saarbrücken, Germany, October 2004.

[35] D. Li, H. Haneda, S. Hishita, and N. Ohashi, "Visible-light-driven nitrogen-doped TiO_2 photocatalysts: effect of nitrogen precursors on their photocatalysis for decomposition of gas-phase organic pollutants," *Materials Science and Engineering B: Solid-State Materials for Advanced Technology*, vol. 117, no. 1, pp. 67–75, 2005.

[36] M. Mrowetz, W. Balcerski, A. J. Colussi, and M. R. Hoffmann, "Oxidative power of nitrogen-doped TiO_2 photocatalysts under visible illumination," *Journal of Physical Chemistry B*, vol. 108, no. 45, pp. 17269–17273, 2004.

[37] Y. Aita, M. Komatsu, S. Yin, and T. Sato, "Phase-compositional control and visible light photocatalytic activity of nitrogen-doped titania via solvothermal process," *Journal of Solid State Chemistry*, vol. 177, no. 9, pp. 3235–3238, 2004.

[38] R. P. Vitiello, J. M. Macak, A. Ghicov, H. Tsuchiya, L. F. P. Dick, and P. Schmuki, "N-Doping of anodic TiO_2 nanotubes using heat treatment in ammonia," *Electrochemistry Communications*, vol. 8, no. 4, pp. 544–548, 2006.

[39] M. Kitano, K. Funatsu, M. Matsuoka, M. Ueshima, and M. Anpo, "Preparation of nitrogen-substituted TiO_2 thin film photocatalysts by the radio frequency magnetron sputtering deposition method and their photocatalytic reactivity under visible light irradiation," *Journal of Physical Chemistry B*, vol. 110, no. 50, pp. 25266–25272, 2006.

[40] S.-K. Joung, T. Amemiya, M. Murabayashi, and K. Itoh, "Relation between photocatalytic activity and preparation conditions for nitrogen-doped visible light-driven TiO_2 photocatalysts," *Applied Catalysis A: General*, vol. 312, no. 1-2, pp. 20–26, 2006.

[41] S. In, A. Orlov, F. García, M. Tikhov, D. S. Wright, and R. M. Lambert, "Efficient visible light-active N-doped TiO_2 photocatalysts by a reproducible and controllable synthetic route," *Chemical Communications*, no. 40, pp. 4236–4238, 2006.

[42] C. Belver, R. Bellod, A. Fuerte, and M. Fernández-García, "Nitrogen-containing TiO_2 photocatalysts. Part 1. Synthesis and solid characterization," *Applied Catalysis B: Environmental*, vol. 65, no. 3-4, pp. 301–308, 2006.

[43] C. Belver, R. Bellod, S. J. Stewart, F. G. Requejo, and M. Fernández-García, "Nitrogen-containing TiO_2 photocatalysts. Part 2. Photocatalytic behavior under sunlight excitation," *Applied Catalysis B: Environmental*, vol. 65, no. 3-4, pp. 309–314, 2006.

[44] T. Matsumoto, N. Iyi, Y. Kaneko, et al., "High visible-light photocatalytic activity of nitrogen-doped titania prepared from layered titania/isostearate nanocomposite," *Catalysis Today*, vol. 120, no. 2, pp. 226–232, 2007.

[45] T. Tachikawa, M. Fujitsuka, and T. Majima, "Mechanistic insight into the TiO_2 photocatalytic reactions: design of new photocatalysts," *Journal of Physical Chemistry C*, vol. 111, no. 14, pp. 5259–5275, 2007.

[46] R. Asahi, Y. Taga, W. Mannstadt, and A. J. Freeman, "Electronic and optical properties of anatase TiO_2," *Physical Review B—Condensed Matter and Materials Physics*, vol. 61, no. 11, pp. 7459–7465, 2000.

[47] C. Di Valentin, G.-F. Pacchioni, and A. Selloni, "Origin of the different photoactivity of N-doped anatase and rutile TiO_2," *Physical Review B—Condensed Matter and Materials Physics*, vol. 70, no. 8, Article ID 085116, 2004.

[48] C. Di Valentin, G.-F. Pacchioni, A. Selloni, S. Livraghi, and E. Giamello, "Characterization of paramagnetic species in N-doped TiO_2 powders by EPR spectroscopy and DFT calculations," *Journal of Physical Chemistry B*, vol. 109, no. 23, pp. 11414–11419, 2005.

[49] K. Yang, Y. Dai, H. Baibiao, and H. Shenghao, "Theoretical study of N-doped TiO_2 rutile crystals," *Journal of Physical Chemistry B*, vol. 110, no. 47, pp. 24011–24014, 2006.

[50] S. Livraghi, M. C. Paganini, E. Giamello, A. Selloni, C. Di Valentin, and G.-F. Pacchioni, "Origin of photoactivity of nitrogen-doped titanium dioxide under visible light," *Journal of the American Chemical Society*, vol. 128, no. 49, pp. 15666–15671, 2006.

[51] S. Livraghi, A. Votta, M. C. Paganini, and E. Giamello, "The nature of paramagnetic species in nitrogen doped TiO_2 active in visible light photocatalysis," *Chemical Communications*, no. 4, pp. 498–500, 2005.

[52] M. A. Henderson, W. S. Epling, C. H. F. Peden, and C. L. Perkins, "Insights into photoexcited electron scavenging processes on TiO_2 obtained from studies of the reaction of O_2 with OH groups adsorbed at electronic defects on $TiO_2(110)$," *Journal of Physical Chemistry B*, vol. 107, no. 2, pp. 534–545, 2003.

[53] T. Berger, M. Sterrer, O. Diwald, et al., "Light-induced charge separation in anatase TiO_2 particles," *Journal of Physical Chemistry B*, vol. 109, no. 13, pp. 6061–6068, 2005.

[54] D. C. Hurum, A. G. Agrios, K. A. Gray, T. Rajh, and M. C. Thurnauer, "Explaining the enhanced photocatalytic activity of degussa P25 mixed-phase TiO_2 using EPR," *Journal of Physical Chemistry B*, vol. 107, no. 19, pp. 4545–4549, 2003.

[55] H. Wang and J. P. Lewis, "Second-generation photocatalytic materials: anion-doped TiO_2," *Journal of Physics Condensed Matter*, vol. 18, no. 2, pp. 421–434, 2006.

[56] J. Pascual, J. Camassel, and H. Mathieu, "Fine structure in the intrinsic absorption edge of titanium dioxide," *Physical Review B*, vol. 18, pp. 5606–5614, 1978.

[57] K. M. Glassford and J. R. Chelikowsky, "Structural and electronic properties of titanium dioxide," *Physical Review B*, vol. 46, pp. 1284–1298, 1992.

[58] R. Sanjines, H. Tang, H. Berger, F. Gozzo, G. Margaritondo, and F. Levy, "Electronic structure of anatase TiO_2 oxide," *Journal of Applied Physics*, vol. 75, pp. 2945–2951, 1994.

[59] H. Tang, F. Levy, H. Berger, and P. E. Schmid, "Urbach tail of anatase TiO_2," *Physical Review B*, vol. 52, pp. 7771–7774, 1995.

[60] S. D. Mo and W. Y. Ching, "Electronic and optical properties of three phases of titanium dioxide: rutile, anatase, and brookite," *Physical Review B*, vol. 51, pp. 13023–13032, 1995.

[61] C. Kim, S. J. Doh, S. G. Lee, S. J. Lee, and H. Y. Kim, "Visible-light absorptivity of a zincoxysulfide (ZnO_xS_{1-x}) composite semiconductor and its photocatalytic activities for degradation of organic pollutants under visible-light irradiation," *Applied Catalysis A: General*, vol. 330, no. 1-2, pp. 127–133, 2007.

[62] V. N. Kuznetsov and N. Serpone, "Visible light absorption by various titanium dioxide specimens," *Journal of Physical Chemistry B*, vol. 110, no. 50, pp. 25203–25209, 2006.

[63] D. Li, N. Ohashi, S. Hishita, T. Kolodiazhnyi, and H. Haneda, "Origin of visible-light-driven photocatalysis: a comparative study on N/F-doped and N-F-codoped TiO_2 powders by means of experimental characterizations and theoretical calculations," *Journal of Solid State Chemistry*, vol. 178, no. 11, pp. 3293–3302, 2005.

[64] J. Wang, W. Zhu, Y. Zhang, and S. Liu, "An efficient two-step technique for nitrogendoped titanium dioxide synthesizing: visible-light-induced photodecomposition of methylene

blue," *The Journal of Physical Chemistry C*, vol. 111, pp. 1010–1014, 2007.

[65] T. Sekiya, K. Ichimura, M. Igarashi, and S. Kurita, "Absorption spectra of anatase TiO_2 single crystals heat-treated under oxygen atmosphere," *Journal of Physics and Chemistry of Solids*, vol. 61, no. 8, pp. 1237–1242, 2000.

[66] T. Sekiya, T. Yagisawa, N. Kamiya, et al., "Defects in anatase TiO_2 single crystal controlled by heat treatments," *Journal of the Physical Society of Japan*, vol. 73, no. 3, pp. 703–710, 2004.

[67] N. Serpone, "Is the band gap of pristine TiO_2 narrowed by anion- and cation-doping of titanium dioxide in second-generation photocatalysts?" *Journal of Physical Chemistry B*, vol. 110, no. 48, pp. 24287–24293, 2006.

[68] J. Chen, L.-B. Lin, and F.-Q. Jing, "Theoretical study of F-type color center in rutile TiO_2," *Journal of Physics and Chemistry of Solids*, vol. 62, no. 7, pp. 1257–1262, 2001.

[69] K. Suriye, P. Praserthdam, and B. Jongsomjit, "Control of Ti^{3+} surface defect on TiO_2 nanocrystal using various calcination atmospheres as the first step for surface defect creation and its application in photocatalysis," *Applied Surface Science*, vol. 253, no. 8, pp. 3849–3855, 2007.

[70] V. N. Kuznetsov and N. Serpone, "Photo-induced coloration and photobleaching of titanium dioxide in TiO_2/polymer compositions on UV- and visible-light excitation into the color centers' absorption bands. Direct experimental evidence negating band gap narrowing in anion-/cation-doped TiO_2," *The Journal of Physical Chemistry C*, vol. 111, pp. 15277–15288, 2007.

[71] A. V. Emeline, N. V. Sheremetyeva, N. V. Khomchenko, V. K. Ryabchuk, and N. Serpone, "Photoinduced formation of defects and nitrogen stabilization of color centers in N-doped titanium dioxide," *Journal of Physical Chemistry C*, vol. 111, no. 30, pp. 11456–11462, 2007.